

Bayesian Nonparametric Common Atoms Regression for Generating Synthetic Controls in Clinical Trials

Noirrit Kiran Chandra^a (noirritchandra@utexas.edu)

Abhra Sarkar^a (abhra.sarkar@utexas.edu)

John F. de Groot^b (john.degroot@ucsf.edu)

Ying Yuan^c (yyuan@mdanderson.org)

Peter Müller^{a,d} (pmueller@math.utexas.edu)

^aDepartment of Statistics and Data Sciences,
The University of Texas at Austin, TX, USA

^bDepartment of Neurological Surgery,
University of California San Francisco, CA, USA

^cDepartment of Biostatistics,
The University of Texas MD Anderson Cancer Center, Houston, TX, USA

^dDepartment of Mathematics,
The University of Texas at Austin, TX, USA

Abstract

The availability of electronic health records (EHR) has opened opportunities to supplement increasingly expensive and difficult to carry out randomized controlled trials (RCT) with evidence from readily available real world data. In this paper, we use EHR data to construct synthetic control arms for treatment-only single arm trials. We propose a novel nonparametric Bayesian common atoms mixture model that allows us to find equivalent population strata in the EHR and the treatment arm and then resample the EHR data to create equivalent patient populations under both the single arm trial and the resampled EHR. Resampling is implemented via a density-free importance sampling scheme. Using the synthetic control arm, inference for the treatment effect can then be carried out using any method available for RCTs. Alternatively the proposed nonparametric Bayesian model allows straightforward model-based inference. In simulation experiments, the proposed method vastly outperforms alternative methods. We apply the method to supplement single arm treatment-only glioblastoma studies with a synthetic control arm based on historical trials.

Key Words: common atoms model, glioblastoma, importance sampling, mixtures, real world data, single-arm trials.

Short/Running Title: Common Atoms Regression Model

Corresponding Author: Noirrit Kiran Chandra (noirritchandra@utexas.edu)

1 Introduction

We introduce a novel Bayesian nonparametric regression model to construct synthetic control arms from external real world data (RWD) to supplement single arm treatment-only trials. The use of common atoms across multiple random probability measures is a critical feature of the proposed construction. Models with similar features have been used before in the literature, including [Denti *et al.* \(2021\)](#); [Camerlenghi *et al.* \(2019\)](#); [Rodríguez *et al.* \(2008\)](#); [Teh *et al.* \(2006\)](#).

Randomized controlled trials (RCT) are the gold standard in evidence-based evaluation of new treatments. RCTs are, however, increasingly associated with bottlenecks involving volunteer recruitment, patient truancy and adverse events ([Nichol *et al.*, 2010](#)) and hence are often very time consuming, expensive and laborious. This is of particular concern for rare diseases, such as glioblastoma (GBM). With digitization of health records and other advances in medical informatics, new data sources are becoming available that can supplement RCTs. For example, relevant information on a control treatment are often available from completed RCTs, electronic health record data, insurance claims data or patient registries from hospitals ([Franklin *et al.*, 2019](#)). Such external data, also referred to as RWD, can augment or substitute the control group in the target clinical trial ([Davi *et al.*, 2020](#)). This has led researchers to consider the creation of synthetic control arms from RWD (see [Schmidli *et al.* 2020](#) for a review). However, the size and heterogeneity of RWD prohibits the direct use of patient level data as a control arm, lest differences with the actual treatment population with respect to patient profiles bias inference on treatment effects ([Burcu *et al.*, 2020](#)). Many existing methods adjust for the lack of randomization in treatment assignments by correcting the bias in the response model and hence can be sensitive to the specification of the treatment assignment as well as the response model as we

discuss below. In this article, we take a fundamentally different approach by resampling a cohort from external health records data that is constructed to be equivalent to the treatment arm in terms of their covariate profiles. The resampled RWD can then serve as the (synthetic) control arm.

There is a fast growing literature on the problem of incorporating RWD in clinical trials. Traditional meta-analytic approaches aim to combine information across studies to construct comparisons of treatments (Sutton and Abrams, 2001). Power prior (Prevost *et al.*, 2000; Chen and Ibrahim, 2000), commensurate prior (Hobbs *et al.*, 2011) and elastic prior (Jiang *et al.*, 2021) constructions leverage available external data to build informative priors from historical data sources. However, these approaches may be inadequate when the RWD population is considerably more heterogeneous than the experimental arm.

Many methods to incorporate RWD in trial design and data analysis are based on propensity scores (PSs), where a PS is defined as the conditional probability of treatment assignment given covariates. In the context of incorporating external data, investigators often use a PS for selection into one or the other data set (rather than for treatment allocation – in case of supplementing a single arm trial with a synthetic control arm these are identical). Rosenbaum and Rubin (1983) showed that an unbiased estimate of the average treatment effect can be obtained by PS adjustments. Most PS-based methods can be broadly classified as using matching, stratification, weighting, or regression. Matching is used to achieve covariate balance across different arms. However, matching propensity scores do not generally imply matching covariates (King and Nielsen, 2019). Stratification splits the data into strata with respect to PSs, and calculates an average treatment effect as a weighted average of within-stratum estimates (Wang *et al.*, 2019; Chen *et al.*, 2020; Lu *et al.*, 2021). However,

PS-stratification may be sensitive to the definition of the strata, and weight-based estimators may be sensitive to the misspecification of the PS model (Zhao, 2004). Regression adjustments, that use the PS as a regressor for the outcome address these issues (Rosenbaum and Rubin, 1983) but the estimates may again be biased if the regression model is misspecified (Vansteelandt and Daniel, 2014). Bayesian nonparametric models that avoid a particular parametric family or structure, such as linearity, of the regression relationship have thus also been proposed (Wang and Rosner, 2019). Nevertheless, consolidated unidimensional PSs can be inadequate in matching multivariate covariates from multiple studies (Stuart, 2010; King and Nielsen, 2019). Additionally, these methods often do not efficiently use all available data by dropping unmatched data. Finally, some other methods (Hasegawa *et al.*, 2017; Li and Song, 2020), although not specifically designed to create synthetic controls, also integrate multiple studies using the covariate distributions.

In this article, we develop an alternative approach based on Bayesian nonparametric (BNP) mixture models. Mixture models imply a random partition of experimental units linked to different atoms in the mixture (Dahl, 2006). We exploit this property to propose a BNP common atoms mixture (CAM) model to introduce matched clusters of patients in a treatment-only trial data set and a (typically much larger) RWD. We show how such matched clusters allow a *density free importance resampling scheme* to generate a subpopulation of the RWD such that the distribution of covariates in the subpopulation can be considered to be equivalent to the single-arm trial. That is, the patients in a matching RWD cluster can be considered *digital clones* of patients in a matching cluster in the single-arm trial.

Inference under the CAM model allows, among others, the following two alternatives to implement inference on treatment effects. Having established equivalent

patient populations, inference can in principle proceed as if treatment had been assigned at random, using inference for RCTs. Alternatively, we propose model-based inference using an extension of the CAM model with a sampling model for the outcome. While both alternatives are based on the same underlying CAM model, we prefer the model-based inference on treatment effect as a more explicit and principled approach.

The proposed CAM model builds on related BNP models in the literature, including the hierarchical Dirichlet process (DP) (Teh *et al.*, 2006) which allows for information sharing across multiple groups through common atoms, the nested DP (Rodríguez *et al.*, 2008) which can identify distributional clusters, and Camerlenghi *et al.* (2019) who proposed a latent mixture of shared and idiosyncratic processes across the sub-models. Denti *et al.* (2021) proposed a CAM model for the analysis of nested datasets where the distributions of the units differ only over a small fraction of the observations sampled from each unit. In contrast to these constructions, the proposed CAM model introduces more structure as needed in our application by setting up two nonparametric Bayesian mixture models with shared atoms and constraints on the implied cluster sizes.

The rest of this paper is organized as follows. Section 2 describes the glioblastoma study that motivated this work. Section 3.1 introduces the proposed common atoms model on the covariates and how it can handle variable dimensional covariates of different data types; Section 3.2 introduces a novel density-free importance resampling scheme to achieve equivalent populations; and Section 3.3 discusses the general common atoms regression model, a flexible mixture of lognormals for censored survival outcomes and an easy to use graphical tool for model validation. In Section 4, we discuss two alternative strategies for inference on treatment effects. Section

5 discusses Markov chain Monte Carlo (MCMC) posterior simulation using a Gibbs sampler. Section 6 presents simulation studies. Section 7 shows results for the motivating GBM data. Section 8 concludes with final remarks. Below, in Table 1, we list the many acronyms used in the paper for easy reference.

Table 1: List of acronyms

Acronym	Full forms	Acronym	Full forms
AUC	area under the receiver operating characteristic curve	IS	importance sampling
BART	Bayesian additive regression tree	KM	Kaplan-Meier
BNP	Bayesian nonparametric	OS	overall survival
CAM	common atoms mixture	PH	proportional hazard
CA-PPMx	common atoms PPMx	PPMx	product partition model with regression on covariates
DP	Dirichlet process	PS	propensity score
GBM	glioblastoma	RCT	randomized controlled trial
HR	hazard ratio	ROC	receiver operating characteristic
		RWD	real-world data
		SOC	standard-of-care

2 Motivating Application in Glioblastoma

Our motivating application arises from a GBM data science project at MD Anderson Cancer Center. GBM is a devastating disease with the average life expectancy of less than 12 months in the general population (Ostrom *et al.*, 2016). Despite decades of intensive clinical research, the progress in developing an effective treatment for GBM lags behind that of other cancers (Aldape *et al.*, 2019). In the last 30 years, only two drugs (carmustine wafers and temozolomide) have been approved by the FDA for patients with newly diagnosed GBM (Fisher and Adamson, 2021). These drugs extend median survival by less than three months and neither offers a potential for cure. One major cause of the high failure rate of the drug development for GBM is suboptimal design of phase II trials, in particular, the common lack of a control arm (Grossman *et al.*, 2017). A review of phase I/II glioblastoma trials from 1980 to 2013 found that

only 20 (5%) were randomized compared to 365 (95%) single-arm trials ([Grossman and Ellsworth, 2016](#)). Reasons for the dominance of single-arm trials include the small number of GBM patients available for clinical trials and investigator’s desire to speed up drug development and reduce trial costs. GBM is a rare disease by the definition of the Orphan Drug Act ([FDA, 2020](#)). Unfortunately, the high heterogeneity of GBM patients makes single-arm trials highly susceptible to bias, contributing to the fact that almost all phase II trials showing promising treatment effects failed in phase III RCTs ([Mandel *et al.*, 2017](#)). The objective of the GBM data science project is to address this pressing issue by leveraging historical data collected at the MD Anderson Cancer Center. The overarching goal is to develop a platform for future single-arm clinical trials in GBM, with synthetic controls constructed from the historical database to enhance the evaluation and screening of new drugs. Working towards this goal, we describe here a method to create synthetic controls, as the engine of the platform, for future trials.

We work with a database that comprises records from 339 highly clinically and molecularly annotated GBM patients treated at MD Anderson over more than 10 years. Once the system is set, the database is expected to be continuously updated with new patient data collected at MD Anderson Cancer Center and potentially combined with the data from other institutions.

After discarding variables with minimal variability across patients and relying on clinical judgment, we identified 11 clinically important categorical covariates. These covariates are commonly considered as prognostic factors in GBM treatments ([Nam and de Groot, 2017](#); [Alexander *et al.*, 2019](#)) and are briefly described in Table 2.

Figure 1 shows the categorical covariates in the historical database and a future treatment-only study which we elaborate in Section 7. Figure S.1 in the supplemen-

tary materials highlights the lack of randomization in the two populations.

Table 2: Description of the covariates in the GBM data.

Covariate	Description
Age	dichotomized at 55 years
KPS	Karnofsky performance score, categorized into three classes: " ≤ 60 ", " $(60, 80]$ " and " > 80 "
RT Dose	radiation therapy dose: dichotomized at 50 Gray
SOC	received standard-of-care (concurrent radiation therapy and temozolomide): Yes/No
CT	participation in a therapeutic trial: Yes/No
MGMT	status of MGMT (<i>O</i> ⁶ -methylguanine-DNA methyltransferase) gene: "methylated", "unmethylated" or "indeterminant"
ATRX	loss of the ATRX chromatin remodeler gene: Yes/No
Gender	gender
EOR	extent of tumor resection: "total", "subtotal" or "laser interstitial thermal therapy" (LITT, Patel and Kim, 2020)
Histologic grade	grade of astrocytoma: IV (GBM) (most cases), or I-III (low-grade or anaplastic) (few)
Surgery reason	"therapeutic" or "other" (relapse)

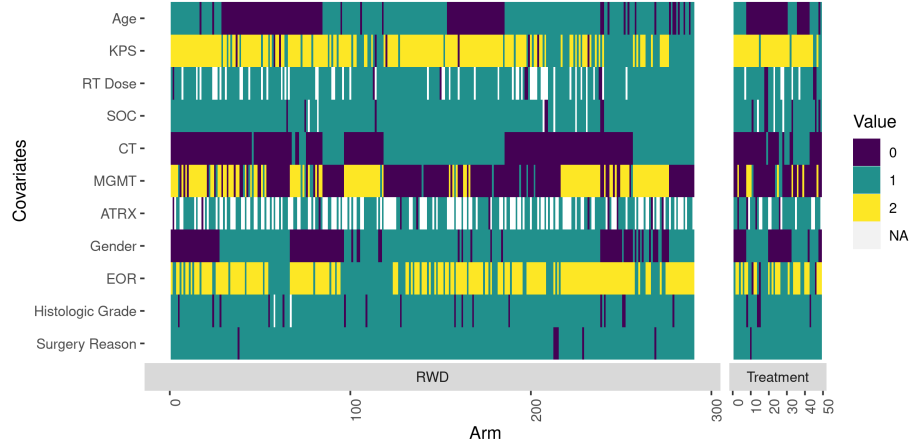


Figure 1: Glioblastoma dataset of 11 baseline categorical covariates with missing entries in the two treatment arms. The left block shows the historical patients. The (smaller) right block shows a hypothetical future trial.

3 Common Atoms Model

We first introduce a model for matching patients with respect to their covariate profiles across different treatment arms and then an extension of the model to include

outcomes. Later we will introduce two alternative methods for inference on treatment effects that build on this model.

3.1 Common Atoms Model on the Covariates

Suppose we have S datasets $(\mathbf{X}_{s,i}, Y_{s,i})$, $s = 1, 2, \dots, S$, with patients $i = 1, \dots, n_s$ associated with a p -dimensional covariate vector $\mathbf{X}_{s,i} = (X_{s,i,1}, \dots, X_{s,i,p})^\top$ and a corresponding response $Y_{s,i}$. In this article, we assume the responses to be univariate. Let $s = 1$ refer to the arm for the (new) treatment of interest, and $s = 2, \dots, S$ denote the RWD datasets. Focusing on the motivating GBM application, we elaborate the model for $S = 2$ with a single RWD set. Extension to multiple RWD's is conceptually straightforward. For each data set s , we denote the sets of covariates and responses by \mathbf{X}_s and \mathbf{Y}_s , respectively, and assume that there are no unmeasured confounders (Baker and Lindeman, 2001; Ventz *et al.*, 2019). For a valid evaluation of treatment effects it is then important to verify equivalent patient populations, i.e., matching distributions of $\mathbf{X}_{s,i}$ under $s = 1$ versus $s = 2$, or to otherwise adjust for any detected difference (Burcu *et al.*, 2020). As the RWD population can be from a variety of sources, such data are typically more heterogeneous than the patient population in the ongoing trial. We develop a novel BNP CAM model with this specific feature to model the two distributions. The proposed CAM model gives rise to a random partition of similar $\mathbf{X}_{1,i}$ and a matching partition of $\mathbf{X}_{2,i}$. Clusters under the latter partition can be considered digital clones of the matching clusters of the earlier partition.

We first construct the model for covariates $\mathbf{X}_{2,i}$ in the RWD. Let $\tilde{\boldsymbol{\zeta}} = \{\tilde{\zeta}_j\}_{j=1}^\infty$ and $\boldsymbol{\pi}_2 = \{\pi_{2,j}\}_{j=1}^\infty$ denote cluster-specific parameters and weights, respectively. We assume

$$\mathbf{X}_{2,i} \mid \boldsymbol{\zeta}, \boldsymbol{\pi}_2 \stackrel{\text{iid}}{\sim} \sum_{j=1}^{\overbrace{\infty}^{F_2}} \pi_{2,j} \mathbf{q}(\mathbf{X}_{2,i} \mid \tilde{\zeta}_j), \quad \tilde{\zeta}_j \mid \boldsymbol{\xi} \stackrel{\text{iid}}{\sim} \bar{\mathbf{q}}(\zeta_j \mid \boldsymbol{\xi}), \quad \boldsymbol{\pi}_2 \sim \text{GEM}(\alpha_2). \quad (1)$$

Here $\mathbf{q}(\cdot \mid \tilde{\zeta}_j)$ is a suitably chosen kernel with parameter $\tilde{\zeta}_j$, $\bar{\mathbf{q}}(\cdot \mid \boldsymbol{\xi})$ is a prior distribution for the $\tilde{\zeta}_j$'s and $\text{GEM}(\alpha)$ is a stick-breaking prior on the mixture weights corresponding to a Dirichlet process with mass parameter $\alpha > 0$ (Sethuraman, 1994). Let $P = \sum \pi_{2,j} \delta_{\tilde{\zeta}_j}(\cdot)$ denote a discrete probability measure with atoms at the $\tilde{\zeta}_j$'s. An equivalent hierarchical model representation of (1) is

$$\mathbf{X}_{2,i} \mid \zeta \stackrel{\text{iid}}{\sim} \mathbf{q}(\mathbf{X}_{2,i} \mid \zeta_i), \quad \zeta_i \mid P \stackrel{\text{iid}}{\sim} P, \quad P \mid \alpha_2, \boldsymbol{\xi} \sim \text{DP}\{\alpha_2, \bar{\mathbf{q}}(\cdot \mid \boldsymbol{\xi})\}, \quad (2)$$

where $\text{DP}(\alpha, P_0)$ is a Dirichlet process with base measure P_0 and mass parameter α (Ferguson, 1973). The discrete nature of the DP random measure P gives rise to possible ties between the ζ_i 's, which defines the desired clusters. For later reference we define notation for these ties and clusters. Introducing latent indicators $c_{2,i}$ with $\mathbf{X}_{2,i} \mid c_{2,i} = j \sim \mathbf{q}(\mathbf{X}_{2,i} \mid \tilde{\zeta}_j)$ and $p(c_{2,i} = j) = \pi_{2,j}$, we have cluster $C_{2,j} = \{i : c_{2,i} = j\}$. Although the DP random probability measure P has infinitely many atoms, only at most n_2 of them are linked with data points $\mathbf{X}_{2,i}$, i.e., this definition of clusters allows for empty clusters C_j . Let ζ_j^* , $j = 1, \dots, k_n$, denote the distinct values of the ζ_i 's, i.e., $\{\tilde{\zeta}_{c_{2,i}}; i = 1, \dots, n_2\} = \{\zeta_1^*, \dots, \zeta_{k_n}^*\}$. We specify the distribution of $\mathbf{X}_{1,i}$ to be a mixture using these same atoms:

$$\mathbf{X}_{1,i} \mid \boldsymbol{\zeta} \stackrel{\text{iid}}{\sim} \sum_{j=1}^{\overbrace{k_n}^{F_1}} \pi_{1,j} \mathbf{q}(\mathbf{X}_{1,i} \mid \zeta_j^*), \quad \boldsymbol{\pi}_1 \sim \text{Dir}\left(\frac{\alpha_1}{k_n}, \dots, \frac{\alpha_1}{k_n}\right), \quad (3)$$

where $\boldsymbol{\pi}_1 = (\pi_{1,1}, \dots, \pi_{1,k_n})$ denotes the probability weights attached to the atoms under F_1 , $\text{Dir}(a_1, \dots, a_r)$ is an r -dimensional Dirichlet distribution with parameters a_1, \dots, a_r , and $\alpha_1 > 0$ is a fixed hyperparameter. Note that model (3) is defined conditionally on (1) and $\mathbf{c}_2 = \{c_{2,i}, i = 1, \dots, n_2\}$ such that \mathbf{X}_1 and \mathbf{X}_2 share the same set of atoms but the distribution of \mathbf{X}_1 is supported only on the non-empty clusters of \mathbf{X}_2 . The motivation behind this construction is that, owing to the bigger size of the RWD compared to the trial arm, \mathbf{X}_2 can be expected to exhibit greater

heterogeneity compared to \mathbf{X}_1 (see, for example, the right panel in Figure 2). The construction avoids the imputation of clusters (strata) with only $\mathbf{X}_{1,i}$'s. There is always a corresponding (non-empty) cluster from the RWD. This is important for the upcoming constructions.

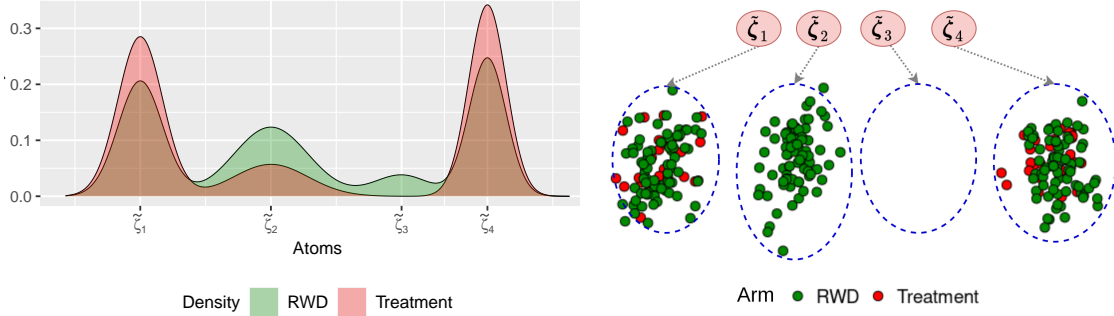


Figure 2: An illustration of the common atoms model: there are a total of four atoms $\tilde{\zeta}_{1:4}$ shared between RWD and the treatment arm. As seen in the right panel, despite having positive weight, the atom $\tilde{\zeta}_3$ is not associated with any sample from the RWD and hence the density on the treatment arm is supported only on the remaining non-empty clusters (left panel). Additionally, the atom $\tilde{\zeta}_2$ is associated with only the RWD. A cluster comprising the treatment arm data alone is however not permissible.

Figure 2 shows a stylized representation of the two mixture models F_1 and F_2 with shared atoms. Notice atom $\tilde{\zeta}_3$ without linked observations and cluster $k = 2$ with only RWD linked to the atom. The $\mathbf{X}_{2,i}$'s linked to $\tilde{\zeta}_1$ and $\tilde{\zeta}_4$ can be regarded as digital clones of the $\mathbf{X}_{1,i}$'s linked to the same atoms.

The described CAM model is different from existing BNP mixture models. In (1)-(3) the atoms linked to \mathbf{X}_2 are always a superset of those atoms that are linked to \mathbf{X}_1 , which is not naturally the case for the hierarchical DP model (Teh *et al.*, 2006). Also, unlike the nested DP (Rodríguez *et al.*, 2008) and common atoms nested DP (Denti *et al.*, 2021) models, there is no notion of clustering distributions. That is, $p(F_1 = F_2) = 0$ a priori. Instead, the intention here is to cluster similar covariate values across the datasets.

An important feature of the proposed CAM model over existing approaches is

the easy use of covariates of different data-types and missing values. Covariates in RCTs often comprise different data-types including continuous, discrete and categorical variables, and missing values are quite common. For example, in Figure 1, a large number of missing values can be observed for the ATRX gene which has only recently been identified as a therapeutic target for glioma (Haase *et al.*, 2018), and was therefore not commonly recorded before.

Many existing methods for handling missing data rely on imputation (Choi *et al.*, 2019) possibly at the expense of an additional layer of prediction errors, or data records with missing variables might be dropped altogether, resulting in reduced sample size. Under the assumption that the missingness is completely at random, the proposed CAM model can avoid this extra structure by accommodating variable dimensional covariates in a principled manner by considering a separate univariate kernel for each covariate. Specifically, let $\mathcal{O}_{s,i} = \{j : X_{s,i,j} \text{ is recorded}\}$ denote the set of observed covariates for patient i in dataset s . We use independent kernels

$$\mathbf{q}(\mathbf{X}_{s,i} \mid \boldsymbol{\zeta}_j^*) = \prod_{\ell \in \mathcal{O}_{s,i}} q_\ell(X_{s,i,\ell} \mid \zeta_{j,\ell}^*), \quad \bar{\mathbf{q}}(\boldsymbol{\zeta}_j^* \mid \boldsymbol{\xi}) = \prod_{\ell=1}^p \bar{q}_\ell(\zeta_{j,\ell}^* \mid \boldsymbol{\xi}), \quad (4)$$

where $q_\ell(\cdot \mid \zeta_{j,\ell}^*)$ is a univariate kernel corresponding to the ℓ^{th} covariate with parameter(s) $\zeta_{j,\ell}^*$ and $\bar{q}_\ell(\zeta_{j,\ell}^* \mid \boldsymbol{\xi})$ is a prior on $\zeta_{j,\ell}^*$ with hyper-parameters $\boldsymbol{\xi}$. The likelihood function of $\mathbf{X}_{s,i}$ is then computed on the basis of only the observed values. The kernel q_ℓ is chosen to accommodate the data-type of the ℓ^{th} covariate. Choice of q_ℓ , \bar{q}_ℓ and associated hyperparameters are elaborated in Section S.5 of the supplementary materials.

3.2 Density-free Importance Resampling of RWD

Building on the fitted CAM on covariates, we propose an importance resampling method to create a subpopulation of \mathbf{X}_2 that can be considered to be equivalent to

\mathbf{X}_1 (see below for a definition of equivalence that is being used here). Under the assumption of no unmeasured confounders, the $\mathbf{X}_{2,i}$'s in the sampled (or weighted) subpopulation can be assumed to follow the same distribution as $\mathbf{X}_{1,i}$, and hence are considered digital clones of the $\mathbf{X}_{1,i}$ who were randomly assigned to control. With such equivalent populations, in principle, any desired method can then be used to carry out inference on treatment effects. Such focus on equivalent populations is strongly recommended by the [FDA \(2021\)](#).

Recall that F_s denotes the mixture model for $\mathbf{X}_{s,i}$, $s = 1, 2$, under models (1) and (3), respectively. We define equivalent populations as a subset (possibly all) of \mathbf{X}_2 together with a set of weights such that expectation of any function of interest $g(\mathbf{X}_{1,i})$ under $\mathbf{X}_{1,i} \sim F_1$ can be evaluated as a (weighted) Monte Carlo average using these \mathbf{X}_2 (and the weights). Here we assume that all stated expectations exist and that expectation and limit can be switched.

Recall that $F_2 = \sum_{h=1}^{\infty} \pi_{2,h} \mathbf{q}(\cdot \mid \tilde{\boldsymbol{\zeta}}_h)$. For easier housekeeping, we assume $\boldsymbol{\zeta}_h^* = \tilde{\boldsymbol{\zeta}}_h$ for $h = 1, \dots, k_n$, i.e., the first k_n atoms are linked with the $\mathbf{X}_{2,i}$'s. Accordingly, we let $F_1 = \sum_{h=1}^{k_n} \pi_{1,h} \mathbf{q}(\cdot \mid \tilde{\boldsymbol{\zeta}}_h)$ using the same first k_n atoms observed in the \mathbf{X}_2 population. This is the exact construction of (1) and (3). For an “*equivalent population*” we require weights w_i attached to $\mathbf{X}_{2,i}$ (using $w_i = 0$ to drop samples), $i = 1, \dots, n_2$ such that the following is satisfied

$$\mathbb{E}_{F_1} \{g(\mathbf{X}_{1,i})\} = \mathbb{E}_{F_2|k_n} \{\hat{g}(\mathbf{X}_2)\} \text{ with } \hat{g}(\mathbf{X}_2) = \sum_{i=1}^{n_2} w_i g(\mathbf{X}_{2,i}),$$

where the expectation on the RHS is with respect to samples $\mathbf{X}_{2,i} \sim F_2 \mid k_n$, $i = 1, \dots, n_2$, subject to being matched with the assumed k_n unique atoms. Recall that $\mathbf{q}(\cdot \mid \tilde{\boldsymbol{\zeta}}_j)$ is the kernel of the j^{th} term in (1). Define $n_{2,j} = |C_{2,j}|$ as the cardinality of the earlier introduced clusters $C_{2,j}$. Then $\frac{1}{n_{2,j}} \sum_{i \in C_{2,j}} g(\mathbf{X}_{2,i})$ is an unbiased estimator of the expectation under $\mathbf{q}(\cdot \mid \tilde{\boldsymbol{\zeta}}_j)$ and

$$\hat{g} = \sum_j \pi_{1,j} \left\{ \sum_{i \in C_{2,j}} \frac{1}{n_{2,j}} g(\mathbf{X}_{2,i}) \right\} = \sum_{i=1}^{n_2} \frac{\pi_{1,c_{2,i}}}{n_{2,c_{2,i}}} g(\mathbf{X}_{2,i})$$

is an unbiased estimator of $\mathbb{E}_{F_1} \{g(\mathbf{X}) \mid \tilde{\boldsymbol{\zeta}}, \boldsymbol{\pi}_1\}$. We recognize then $\pi_{1,c_{2,i}}/n_{2,c_{2,i}}$ as the ideal weights. Replacing $\pi_{1,c_{2,i}}/n_{2,c_{2,i}}$ in \hat{g} by a Monte Carlo average under a suitable posterior MCMC simulation, we get the desired equality simulation-exact (as n_1, n_2 and the number of MCMC simulations increases). Let $m = 1, \dots, M$ index the posterior Monte Carlo sample and use $\pi_{1,j}^{(m)}$, $n_{2,j}^{(m)}$, etc. to indicate parameter values in the m^{th} Monte Carlo sample. We use

$$\hat{g} = \sum_i w_i g(\mathbf{X}_{2,i}), \quad w_i \propto \sum_{m=1}^M \pi_{1,c_{2,i}}^{(m)} / n_{2,c_{2,i}}^{(m)}, \quad (5)$$

with w_i being the *importance sampling* weight for $\mathbf{X}_{2,i}$. The $\mathbf{X}_{2,i}$'s can be resampled with these weights to obtain the desired subpopulation with distribution $F_1(\mathbf{x})$ (Skare *et al.*, 2003). This resampled subpopulation of \mathbf{X}_2 can then be regarded as equivalent in distribution to \mathbf{X}_1 . Algorithm 1 summarizes the procedure.

Algorithm 1: Density-free importance resampling of RWD and validation

- 1 **Input** two data sets \mathbf{X}_1 and \mathbf{X}_2 .
 - 2 **Fit CAM** to the data using MCMC with M iterations. Let $\boldsymbol{\pi}_1^{(m)}$ and $\mathbf{c}_2^{(m)}$ be the m^{th} MCMC sample of $\boldsymbol{\pi}_1$ and \mathbf{c}_2 , respectively, and $n_{2,j}^{(m)}$ be the size of cluster $C_{2,j}$ in the m^{th} MCMC iteration for $m = 1, \dots, M$.
 - 3 **Calculate** the importance sampling weights $w_i \propto \sum_{m=1}^M \pi_{1,c_{2,i}}^{(m)} / n_{2,c_{2,i}}^{(m)}$ for $i = 1, \dots, n_2$.
 - 4 **Resample** a subpopulation of size n_1 from \mathbf{X}_2 with importance resampling weights w_i with replacement.
 - 5 **Test for equivalence** of \mathbf{X}_1 and the resampled subpopulation of \mathbf{X}_2 using a supervised classification algorithm (for example, a BART random forest as described in the text).
-

In our implementation of Step 5 of Algorithm 1, we use a Bayesian additive regression tree (BART, Chipman *et al.*, 2010). In extensive simulation studies in Section 6, we notice that an AUC (area under the receiver operating character characteris-

tic curve) less than 0.6 yields excellent empirical performance. Once equivalence is achieved, in principle any existing approach for inference on treatment effects can be used (see Section 4 and later).

In general, importance sampling schemes need the ratio of the target density (in our case, F_1) and the importance sampling density (F_2). In our case, this would require impossible high-dimensional density estimation. Even if densities were known, importance sampling would be plagued by unbounded weights (Au and Beck, 2003). Exploiting the common atoms structure, the proposed scheme does not require evaluation of the marginal multivariate densities. We therefore refer to this as a *density-free importance resampling* scheme. The use of the Rao-Blackwellization implemented by the use of $n_{2,j}$ in the denominator of w_i avoids complications arising from unbounded weights. By definition the denominator in (5) is bounded by 1 from below.

3.3 Regression with CAM Model on Covariates

Note that up to here we only concerned ourselves with $F_s(\mathbf{X})$, without any reference to the outcomes \mathbf{Y} . In preparation for one of the strategies in the upcoming discussion of treatment comparison (Section 4), we now augment the CAM model to include a sampling model for the outcomes. That is, we add a response model on top of the CAM model on covariates.

The extended model defines a regression of $Y_{s,i}$ on covariates $\mathbf{X}_{s,i}$ by first specifying a random partition that groups patients with similar covariate profiles in clusters implied under the CAM model (1) and (3), and then adding a cluster-specific sampling model for the outcome $Y_{s,i}$. That is, the overall model specifies a regression of $Y_{s,i}$ on $\mathbf{X}_{s,i}$ via random partition. A major advantage of this approach is that it allows a variable-dimension covariate vector – a feature that is not straightforward to include in

a regression otherwise. Similar product partition models with regression on covariates (PPMx, see also S.2 in the supplementary materials) were considered earlier by Müller *et al.* (2011) and Page *et al.* (2021), albeit without any notion of common atoms. We will therefore refer to the model proposed below as the common atoms PPMx (CA-PPMx). Formally, letting $\boldsymbol{\theta}_s = (\boldsymbol{\theta}_{s,j}; j = 1, \dots, k_n)$ be cluster specific parameters for $s = 1$ and 2, we assume

$$(Y_{s,i} \mid \boldsymbol{\theta}_s, c_{s,i} = j) \stackrel{\text{ind}}{\sim} h(Y_{s,i} \mid \boldsymbol{\theta}_{s,j}), \quad (6)$$

for a suitable choice of h . For example, h could be a lognormal, exponential or Weibull model for an event-time response. The response model (6) depends on the covariates indirectly via $c_{s,i}$'s, i.e., the partition induced by the covariates. Within stratum $C_j = C_{1,j} \cup C_{2,j}$, the response models allows for a treatment comparison based on $(\boldsymbol{\theta}_{1,j}, \boldsymbol{\theta}_{2,j})$, which can then be averaged with respect to some assumed distribution on $\mathbf{X}_{s,j}$. We discuss details later, in the next subsection. Alternatively, we find a marginal outcome model, marginalized with respect to $\mathbf{X}_{s,j}$, by integrating out the cluster indicator variables, to obtain

$$(Y_{s,i} \mid \boldsymbol{\theta}_s, \boldsymbol{\pi}_s) \sim f_s(Y_{s,i} \mid \boldsymbol{\theta}_s, \boldsymbol{\pi}_s) = \sum_{j=1}^{\infty} \pi_{s,j} h(Y_{s,i} \mid \boldsymbol{\theta}_{s,j}), \quad (7)$$

where we set $\pi_{1,j} = 0$ for all $j > k_n$ to simplify notations. Note that, as a byproduct of the model fit, one gets the same weights $\boldsymbol{\pi}_1$ (and \mathbf{c}_2) that were used for the importance resampling scheme in Section 3.2.

For the implementation in the motivating case study, we let $Y_{s,i}$ denote the log OS (overall survival) times and assume $h(Y_{s,i} \mid \boldsymbol{\theta}_{s,j})$ to be a normal kernel with $\boldsymbol{\theta}_{s,j} = (\mu_{s,j}, \sigma_{s,j}^2)$. Such mixtures provide a highly flexible likelihood model (Ghosal *et al.*, 1999), making them an attractive choice for many applications. We complete the model with conjugate normal-inverse-gamma (NIG) priors on the $(\mu_{s,j}, \sigma_{s,j}^2)$'s. In summary,

$$Y_{s,i} \mid c_{s,i} = j, \boldsymbol{\theta}_s \stackrel{\text{ind}}{\sim} \text{N}(\mu_{s,j}, \sigma_{s,j}^2), \mu_{s,j} \mid \sigma_{s,j}^2 \stackrel{\text{ind}}{\sim} \text{N}\left(\mu_0, \frac{\sigma_{s,j}^2}{\kappa_0}\right), \sigma_{s,j}^{-2} \stackrel{\text{iid}}{\sim} \text{Ga}(a_0, b_0), \quad (8)$$

where $\text{Ga}(a_0, b_0)$ is a gamma distribution with mean a_0/b_0 and variance a_0/b_0^2 . We add the hyper-priors $\mu_0 \sim \text{N}(m_\mu, s_\mu^2)$ and $\log b_0 \sim \text{N}(m_b, s_b^2)$, on the main location-scale controlling hyper-parameters μ_0 and b_0 while fixing the precision hyper-parameters κ_0 and a_0 at values ensuring a weakly informative prior. The choice of these hyper-parameters are discussed in Section S.5 of the supplementary materials.

Test of fit: For a goodness-of-fit test under the proposed model, we generalize the approach by Johnson (2007) and build a graphical quantile plot based tool to assess the model fit. Such visual tools are quite effective for detecting departures from model assumptions (Meloun and Militký, 2011, Chapter 2). Details are described in Section S.3 of the supplementary materials for space constraints.

4 Inference on Treatment Effects

We introduce two alternative methods for inference on treatment effects. One makes use of the density-free IS scheme of Section 3.2 while the other builds on the response model of Section 3.3.

4.1 Two-step Importance Sampling (IS) Approach

We already described the use of the weights $\pi_{s,j}$ in the CAM model to achieve equivalent patient populations. We did this in preparation for a straightforward approach to treatment comparison. Using the adjusted (resampled) subpopulation of \mathbf{X}_2 , one can proceed with inference on the treatment effect using any method relying on equivalent patient populations across the two arms. We refer to this approach as the “two-step

IS” as one of the methods for inference, and use it in the simulation studies and applications in Sections 6 and 7, respectively. Note that this approach does not make use of the outcome model of Section 3.3.

4.2 Model-Based Inference for Treatment Effects

Alternatively, we implement inference using the response model of Section 3.3, i.e., the full CA-PPMx. We refer to this approach as **“model-based inference”**. We assume that the desired inference on treatment effects takes the form of inference for some notion of difference $\delta(\cdot, \cdot)$ of the marginal distributions under the two treatment arms, $\Delta_\theta = \delta\{f_1(\cdot \mid \boldsymbol{\theta}_1, \boldsymbol{\pi}_1), f_2(\cdot \mid \boldsymbol{\theta}_2, \boldsymbol{\pi}_2)\}$. However, since the covariate populations in the two treatment arms are substantially different, comparison between the marginal (with respect to the covariates) outcome models $f_1(\mathbf{Y}_{1,i} \mid \boldsymbol{\theta}_1, \boldsymbol{\pi}_1)$ and $f_2(\mathbf{Y}_{2,i} \mid \boldsymbol{\theta}_2, \boldsymbol{\pi}_2)$ can be biased. We need to appropriately adjust for the differences in the two populations. Exploiting the common atoms structure of the proposed CA-PPMx, there is an operationally simple method to carry out this adjustment and infer treatment effects. Since within each cluster, the covariate populations can be considered equivalent, the adjustment for the lack of randomization amounts to adjusting the corresponding cluster weights. We define

$$\tilde{f}_2(Y \mid \boldsymbol{\theta}_2, \boldsymbol{\pi}_1) = \sum_{j=1}^{k_n} \pi_{1,j} h(Y \mid \boldsymbol{\theta}_{2,j}),$$

where the mixture components $h(Y \mid \boldsymbol{\theta}_{2,j})$ of the response model in the RWD are weighted by $\boldsymbol{\pi}_1$, i.e., the cluster weights associated with \mathbf{X}_1 (rather than $\boldsymbol{\pi}_2$). Thus, \tilde{f}_2 is the distribution of outcomes under control in the treatment population or, in other words, the response of an average individual from the trial arm potentially treated with the control therapy. With these notions, we define the population adjusted treatment effect as

$$\tilde{\Delta}_\theta = \delta\{f_1(\cdot \mid \boldsymbol{\theta}_1, \boldsymbol{\pi}_1), \tilde{f}_2(\cdot \mid \boldsymbol{\theta}_2, \boldsymbol{\pi}_1)\}. \quad (9)$$

From the posterior distribution of $\tilde{\Delta}_\theta$, inference can be straightforwardly carried out. We refer to this approach of evaluating the treatment effect as CA-PPMx (naming it after the underlying extended CAM model). For example, consider Y being a univariate real-valued response variables and $\delta(f_1, f_2) = \mathbb{E}_{f_1}(Y) - \mathbb{E}_{f_2}(Y)$. Then the treatment effect $\tilde{\Delta}_\theta$ simplifies to $\tilde{\Delta}_\theta = \sum_{j=1}^{k_n} \pi_{1,j} \{ \mathbb{E}_{h(Y|\boldsymbol{\theta}_{1,j})}(Y) - \mathbb{E}_{h(Y|\boldsymbol{\theta}_{2,j})}(Y) \}$.

Note that each cluster of covariates in the CAM model can be interpreted as a homogeneous group of patients. For the j^{th} group, the average treatment effect is $\mathbb{E}_{h(Y|\boldsymbol{\theta}_{1,j})}(Y) - \mathbb{E}_{h(Y|\boldsymbol{\theta}_{2,j})}(Y)$ and its proportion in the treatment arm is $\pi_{1,j}$. The weighted average $\tilde{\Delta}_\theta$ therefore represents the overall mean difference in effects between the actual experimental therapy and the potential control therapy for the patients in the treatment arm. In general, a similar simplification holds whenever $\delta(f_1, f_2)$ takes the form of a difference in expectations of some linear function $T(\cdot)$ under f_1 versus f_2 and we can write

$$\tilde{\Delta}_\theta = \sum \pi_{1,j} [\mathbb{E}_{h(Y|\boldsymbol{\theta}_{1,j})} \{ T(Y) \} - \mathbb{E}_{h(Y|\boldsymbol{\theta}_{2,j})} \{ T(Y) \}] . \quad (10)$$

In the common case $\boldsymbol{\theta} = \mathbb{E}_{h(Y|\boldsymbol{\theta})} \{ T(Y) \}$, the treatment effect further simplifies to $\tilde{\Delta}_\theta = \sum \pi_{1,j} (\boldsymbol{\theta}_{1,j} - \boldsymbol{\theta}_{2,j})$.

See Section S.4 in the supplementary materials for an interpretation of the proposed model-based inference on treatment effects in the CA-PPMx model as a stochastic propensity score stratification approach.

We prefer the Bayesian model-based approach to avoid discarding unmatched patient records from the RWD from the analysis. Nevertheless, the two-step IS can be quite useful to validate the results obtained by the model-based approach.

5 Posterior Computation

We develop an efficient and operationally simple Gibbs sampling algorithm for posterior inference in the proposed CAM model for non-conjugate mixture of lognormals on survival outcomes. One potential complication arises from the dimension of $\boldsymbol{\pi}_1$, which vary depending on the observed atoms in \mathbf{X}_2 . Posterior simulation with variable dimensional parameters generally involves complicated trans-dimensional Monte Carlo simulation (Green, 1995) often resulting in poor mixing and computational inefficiencies. Our posterior sampling algorithm avoids such complications while rigorously maintaining the architecture of the CAM model. Section S.6 in the supplementary materials for more details.

6 Simulation Study

We set up simulation studies to compare the CA-PPMx model with the propensity score-integrated power prior (Wang *et al.*, 2019) and composite likelihood approach (Chen *et al.*, 2020) which we have implemented using the `psrwe` R package. We first describe the simulation scenarios.

CAM scenario: We first consider a scenario where the covariates are generated from a CAM model. In this scenario, we take the first $q = \lfloor p/2 \rfloor$ covariates to be continuous and the remaining $(p - q)$ covariates to be binary. For the trial arm $s = 1$, we generate $\mathbf{X}_{1,i,1:q} \stackrel{\text{iid}}{\sim} N_q(\boldsymbol{\mu}_1, \sigma_1^2 \mathbf{I}_q)$ and $X_{1,i,\ell} \stackrel{\text{iid}}{\sim} \text{Bernoulli}(\varrho_1)$ for $\ell = q+1, \dots, p$. For the RWD arm, $s = 2$, we generate $\mathbf{X}_{2,i,1:q} \stackrel{\text{iid}}{\sim} \sum_{j=1}^2 \pi_j N_q(\boldsymbol{\mu}_j, \sigma_j^2 \mathbf{I}_q)$ and $X_{2,i,\ell} \stackrel{\text{iid}}{\sim} \sum_{j=1}^2 \pi_j \text{Bernoulli}(\varrho_j)$ for $\ell = q+1, \dots, p$ with $\pi_1 \ll \pi_2$ ensuring that the \mathbf{X}_2 population is substantially different to \mathbf{X}_1 in having more heterogeneity.

MIX scenario: In another scenario, we generate $\mathbf{X}_{1,i} \stackrel{\text{iid}}{\sim} \sum_{j=1}^k \pi_{1,j} N_p(\boldsymbol{\mu}_j, \sigma^2 \mathbf{I}_p)$ and

$\mathbf{X}_{2,i} \stackrel{\text{iid}}{\sim} \sum_{j=1}^{k-1} \pi_{2,j} \mathbf{N}_p(\boldsymbol{\mu}_j, \sigma^2 \mathbf{I}_p)$. Different weights attached to the atoms and the extra k^{th} atom in the \mathbf{X}_1 population result in significantly different marginal densities of the two populations. Here the RWD includes fewer atoms in the mixture than the treatment arm. Given the typically larger heterogeneity of the RWD this is not a very realistic scenario and, in fact, is opposite to the assumed analysis model. We include this scenario as a model misspecification scenario.

Interaction scenario: In this scenario, we resample from the historical GBM database of 339 patients to create a future single-arm trial population. Let $F(\mathbf{X})$ denote the (unknown) distribution of the covariates in the database, and Z be the corresponding indicator variable such that $Z = s$ if and only if \mathbf{X} is assigned to the treatment arm s . We then sample $\mathbf{X}_{1,i}$ i.i.d. from $p(\mathbf{X}_{1,i}) \propto F(\mathbf{X}_{1,i}) \cdot e(\mathbf{X}_{1,i})$ and $\mathbf{X}_{2,i}$ from $p(\mathbf{X}_{2,i}) \propto F(\mathbf{X}_{2,i}) \cdot \{1 - e(\mathbf{X}_{2,i})\}$ where $e(\mathbf{X}) = \Pr(Z = 1 \mid \mathbf{X})$ is the PS of assignment to the treatment arm. We define $e(\mathbf{X})$ as a logistic regression with interactions between covariates. Note that we can sample $\mathbf{X}_{s,i}$ by simple weighted resampling of the historical database, without explicitly knowing $F(\cdot)$.

Oracle scenario: In this fourth scenario we proceed as in the Interaction scenario, but now with $e(\mathbf{X})$ defined as a logistic regression with main effects for the covariates only. That is, as if an oracle had revealed the right predictors for the logistic function.

Outcome model: The `psrwe` package includes the option of a Gaussian response model alone. Therefore, in all four scenarios we generate $Y_{1,i} = \delta + \mathbf{X}_{1,i}^T \boldsymbol{\beta} + \epsilon_{1,i}$ and $Y_{2,i} = \mathbf{X}_{2,i}^T \boldsymbol{\beta} + \epsilon_{2,i}$, where $\epsilon_{s,i} \stackrel{\text{iid}}{\sim} \mathbf{N}(0, \tilde{\sigma}^2)$ for $i = 1, \dots, n_s$ and $s = 1, 2$, implying δ as the true treatment effect. We repeat the experiments for $\delta = -1, 0, 1, 3, 5$.

We repeat the simulations in the CAM and MIX scenarios for $p = 10, 15, 20$, $n_1 = 50, 100, 150$ and set $n_2 = 6 \times n_1$ for all setups, keeping the ratio of the population sizes consistent with the GBM application. For each (n_1, p, δ) combination in the

CAM and MIX scenarios, we perform 100 independent replications. In the last two scenarios, there are $p = 11$ covariates and we use $n_1 = 49$. Also, to avoid reporting summaries that might just hinge on a lucky choice of the logistic regression coefficients in $e(\cdot)$ and to remove one source of randomness unrelated to the methods under comparison, we independently sample a different set of regression coefficients (from a discrete mixture distribution) for each of the 100 repeat simulations.

Analyses: We perform six different analyses for each of the four scenarios to estimate the treatment effect Δ_θ which we define here as the difference in mean outcomes, i.e., the simulation truth δ . The analyses are (i) CA-PPMx, an analysis using the proposed *CA-PPMx* model of Section 4.2; (ii) the two-step IS approach introduced in Section 3.2. We first sample a subpopulation of size n_1 from \mathbf{X}_2 following the importance resampling scheme proposed in Section 3.2 and subsequently estimate the treatment effect between the subpopulation and the treatment arm by fitting a linear model. We refer to this analysis as *IS-LM*; (iii) and (iv) two PS-based power prior approaches using a logistic model and random forest (Breiman, 2001), respectively. We refer to these analyses as *PP-Logistic* and *PP-RF*, respectively; and finally, (v) and (vi) two composite likelihood approaches with logistic and random forest classifier based PSs, referred to here as *CL-Logistic* and *CL-RF*, respectively. Under the Interaction and Oracle scenarios, random forest-based PS methods as implemented in the `psrwe` package were very unstable. We therefore do not include them in the summaries below.

Equivalence of populations: In preparation for inference under the two-step IS approach, we generate equivalent populations using the density-free importance resampling scheme discussed in Section 3.2 based on the fitted CAM model. To formally

test for equivalence of the adjusted datasets we implement Step 5 in Algorithm 1. We first merge the datasets and then try to classify patients in the merged sample as originally RWD or single-arm treatment cohort ($s = 2$ vs. $s = 1$, in the earlier notation). For classification, we use BART and report the boxplots of the area under the receiver operating characteristic curve (AUC) of the classification accuracy across the independent experiments for all simulation settings in Figure 3. For comparison, we also subsample randomly (instead of using the IS weights) and report the AUCs in the same figure. We refer to the two sampling strategies as *IS* and *Random*, respectively.

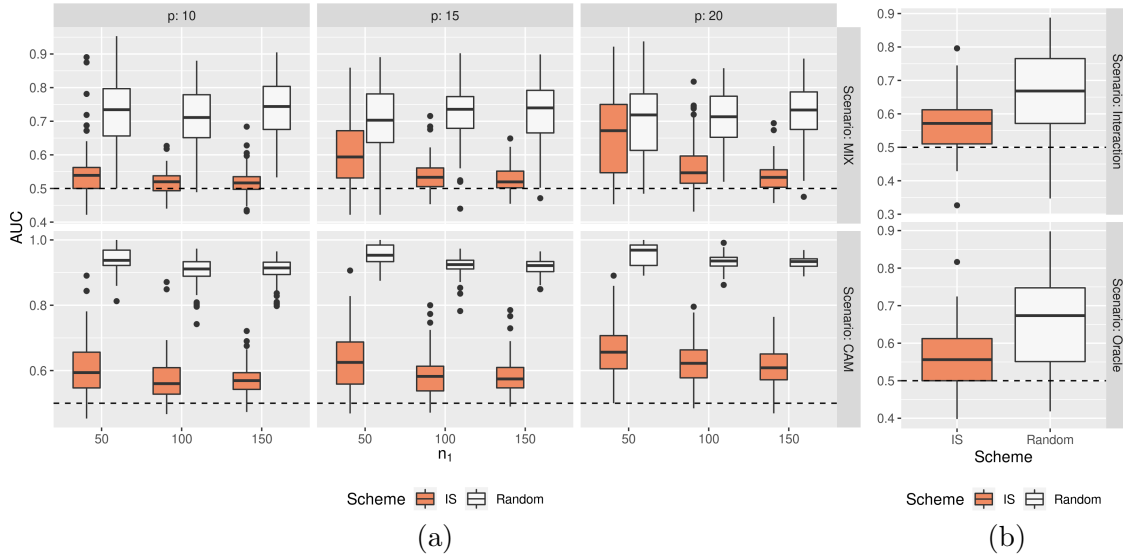


Figure 3: Boxplots of the area under the receiver operating characteristic curve (AUC) of the classification accuracy for a merged dataset consisting of \mathbf{X}_1 and the subsampled \mathbf{X}_2 using BART, and trying to classify into originally \mathbf{X}_1 versus \mathbf{X}_2 . Two subsampling schemes are used - the importance sampling (IS) strategy in Section 3.2 and simple random resampling. Here AUCs close to 0.5 implies near equivalence between the populations. Panel (a) shows the AUCs in the CAM and MIX scenarios across different sample sizes and number of covariates; and (b) shows the AUCs under the Interaction and Oracle scenarios.

In Figure 3(a) the Random resampling strategy yields quite high AUC indicating that the two populations are substantially different and adjustment in the RWD population is necessary before using it as synthetic control. For both CAM and MIX scenarios, the performance of the IS scheme improves with increasing sample size but

deteriorates with the number of covariates. This is expected as for small sample sizes \mathbf{X}_2 is lacking enough data to produce a subsample equivalent to \mathbf{X}_1 .

Under the CAM scenario, the Random scheme yields AUCs of nearly 1, implying that the true populations are indeed very different in this case. This also explains the slightly higher AUCs that can be observed under this scenario (compared even to the model misspecification scenario MIX). Although not perfect, AUCs very close to 0.5 for the IS scheme implies near equivalence between the populations. In both of these scenarios, substantially lower AUCs were obtained by the IS resampling scheme, implying that the proposed CAM model indeed adjusts for the lack of randomization.

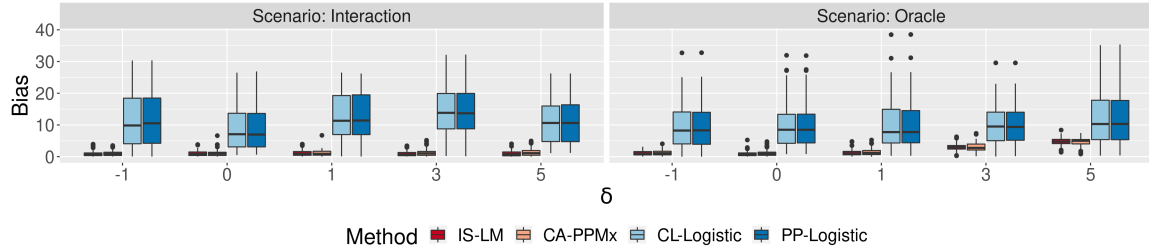
Results under the last two scenarios are shown in Figure 3(b). Recall that in both scenarios the simulation truth is not based on the CAM model. Still, the fit under the proposed CAM model facilitates near perfect adjustment as shown in the figure.

Inference on treatment effects: Boxplots of the biases in estimating the treatment effect δ , i.e., difference to the true treatment effect in each simulation setup, are provided in Figure 4. Estimated treatment effects under CA-PPMx are evaluated using the posterior mean of (9). Two-step IS-LM and CA-PPMx uniformly outperforms the PS based methods. Performance of the approaches based on the common atoms model improve with increasing sample size. The same is not the case for the other methods, possibly indicating that these latter methods may require a much larger population size in the RWD to adjust for the lack of randomization.

Interestingly the two-step IS-LM performs better than the fully Bayesian model-based CA-PPMx in the simulation experiments. The IS-LM is favored since the simulation truth of the response model is in fact linear and parametric models usually are more powerful than nonparametric ones under true model specification.



(a) CAM (top) and MIX (bottom) scenarios



(b) Interaction (left) and oracle (right) scenarios.

Figure 4: Biases in estimating treatment effects: Boxplots of the biases across the 100 independent replicates are provided for each simulation setup. Six methods are used to estimate the effects where IS-LM and CA-PPMx are based on the proposed CAM model and the rest are PS based approaches. Panels (a) correspond to the simulation scenarios CAM and MIX in the top and bottom figures, respectively. Panel (b) shows results under the interaction (left side) and the oracle (right side) scenarios.

7 Application in Glioblastoma

We return to the motivating case study of creating a synthetic control for an hypothetical upcoming single-arm GBM trial. The sample size of the trial is $n_1 = 49$, similar to past trials (Vanderbeek *et al.*, 2018). The endpoint of interest is OS. We evaluate the operating characteristics of the proposed design by simulating $L = 100$ trial replicates. See Berry *et al.* (2010, Section 2.5.4) for a discussion of the role of frequentist operating characteristics in Bayesian inference. To create the treatment arm data, we first select covariates $\mathbf{X}_{1,i}$ by randomly selecting patients from the historical database. To generate a realistic non-equivalent patient population, we selected not uniformly but using a logistic regression on the covariates (as described in the Interaction scenario in Section 6). The treatment effect is quantified by the hazard ratio (HR) between the treatment arm and the (synthetic) control arm, with the null and alternative hypotheses $H_0 : \text{HR} = 1$ vs. $H_1 : \text{HR} \leq 0.6$ at a time 50 weeks. The HR of 0.6 was suggested by clinical collaborators as a clinically meaningful target.

We show results under two alternative scenarios (a) H_0 : no treatment effect (i.e., $\text{HR} = 1$), created by keeping OS for the patients in the treatment arm as was originally observed in the historical database (since the patients received treatments with similar efficacy); and (b) H_1 : there is a clinically meaningful treatment effect. We created H_1 by increasing OS of patients in the treatment arm with an increment that would correspond to a HR of 0.6 under an exponential model.

We apply two methods to make inference on the treatment effect: (i) the two-step IS procedure, where we first create equivalent patient populations using Algorithm 1 from Section 3.2; and then proceed with inference on the treatment effect as if patients were randomly assigned to treatment and control; and (ii) the model-based inference with an extension of the CAM model to include the outcomes $Y_{s,i}$, as described in

Section 4.2.

(i) **Two-step IS procedure:** In preparation for inference, we start with a test for equivalence of the subsampled population in each of the $L = 100$ repeat simulations.

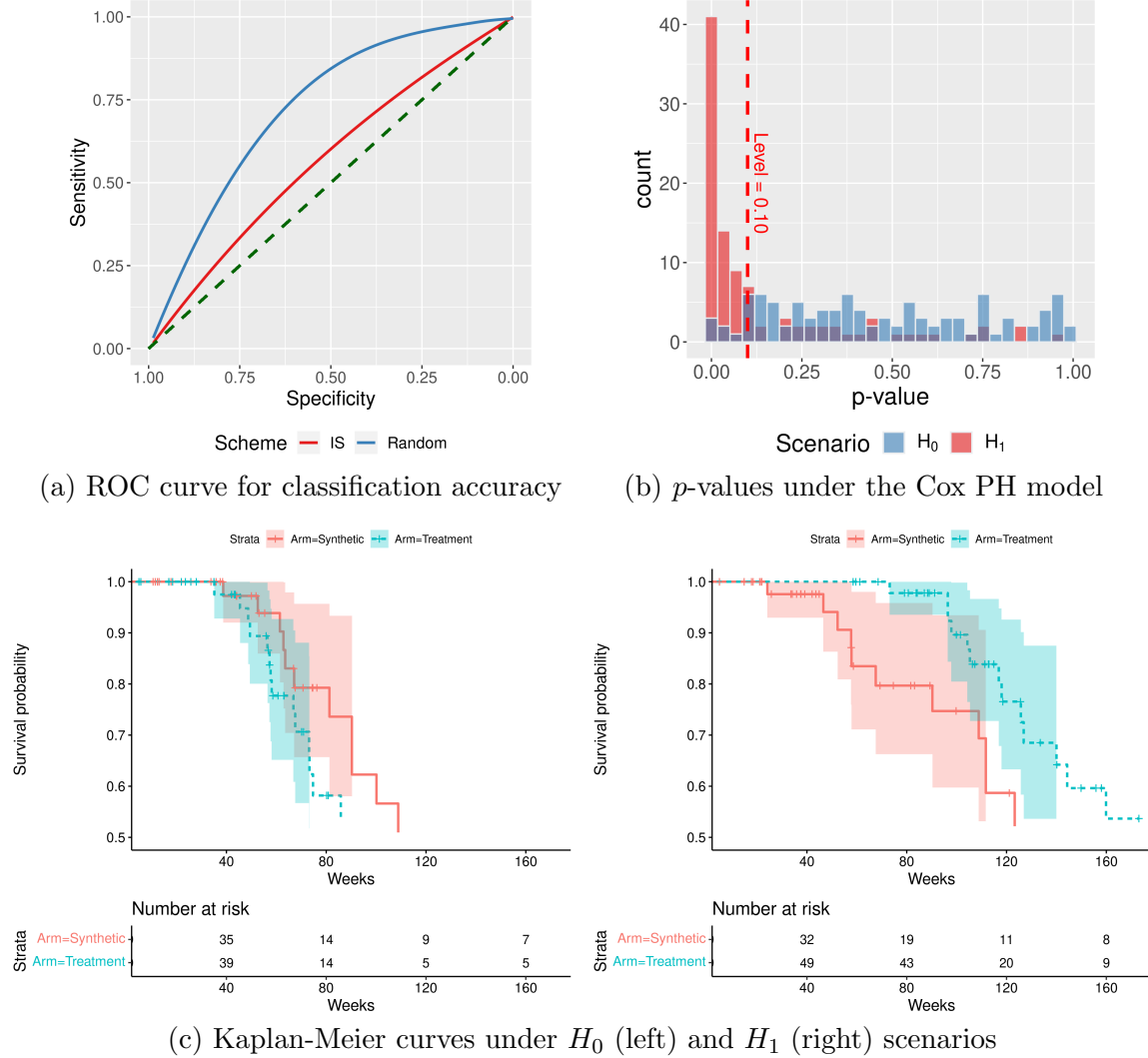


Figure 5: Inference under treatment effects under the two-step IS procedure: Panel (a) shows the ROC curves of classification accuracy between the covariates in the treatment arm and the subsampled RWD using BART in the two-step IS strategy of Section 3.2 (red line) and using random resampling (blue curve); panel (b) shows histograms of the p -values corresponding to a logrank test under the Cox PH model comparing the survival curves between the treatment arms; and panel (c) shows the Kaplan-Meier curves and pointwise confidence intervals for treatment (blue) and control (red) arms under scenarios H_0 (left) and H_1 , respectively.

In Figure 5(a), we plot the receiver operating characteristic (ROC) curves for

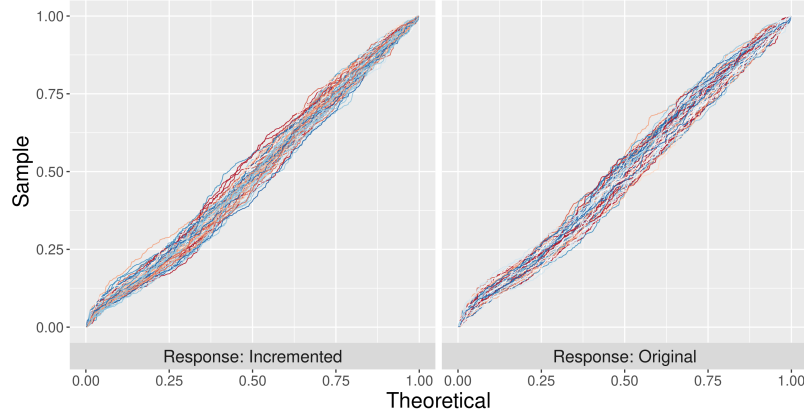
the classification of the merged sample into originally treatment arm versus adjusted RWD (Step 5 in Algorithm 1) (almost diagonal red line). For comparison, we also show the ROC curve under random sampling (blue, bent curve). The strictly non-linear blue ROC curve under random sampling shows that the covariate populations are indeed different. The almost diagonal ROC curve under the proposed IS scheme demonstrates that the scheme did indeed adjust for differences in the two groups.

Once we establish equivalence of the patient populations, we proceed with inference for the treatment effect. We use a Cox proportional hazard (PH) model (Cox, 1972) and the logrank test (Peto and Peto, 1972) to compare the survival functions. Figure 5(b) shows inference summaries over the $L = 100$ repetitions. The figure shows histograms of p -values under H_0 (in blue) and H_1 (in red). Under H_0 , p -values are almost uniformly spread out over $[0, 1]$. In contrast, under H_1 the histogram of p -values over repeat simulations is peaked close to zero.

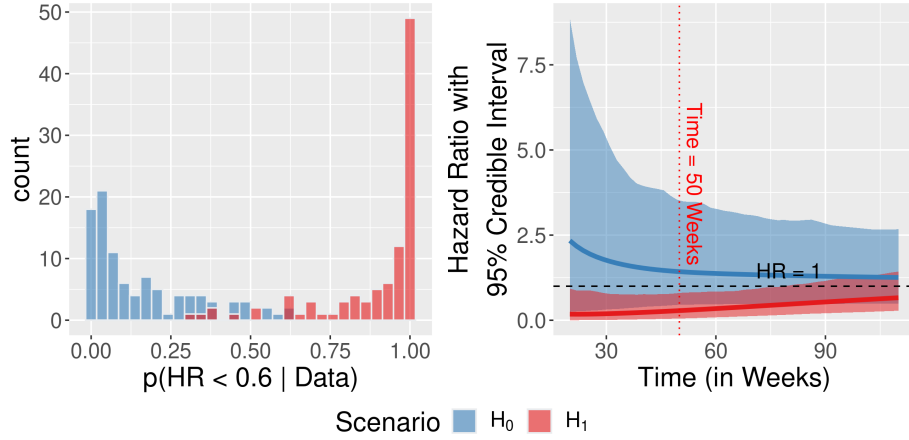
Finally, we identify representative simulations from the L repetitions under each of the two scenarios by finding the simulation with p -value closest to the median of the respective histogram. For those two selected repetitions, we show Kaplan-Meier plots for the survival curves in the left and right panels of Figure 5(c), respectively. We observe that for the original OSs, the survival curves in the two arms are quite alike with wide confidence intervals, whereas for the incremented responses significant improvements in the survival times can be observed for the treatment arm for the first 80 weeks.

(ii) Model-based inference: For model-based inference on treatment effects, we first assess goodness-of-fit of the CA-PPMx model (see Section S.3 in the supplementary materials for details). Quantile-quantile plots for the two scenarios are shown in

Figure 6(a). Near diagonal lines indicate no evidence for a lack of fit. We then report



(a) QQ plots for goodness of fit where deviance from the diagonal line indicates a lack of fit



(b) $p(H_1 | \text{Data})$ (left) and hazard ratio with 95% posterior credible interval (right)

Figure 6: Inference under treatment effects under the model-based approach: Panel (a) shows quantile-quantile plots to assess model fit as elaborated in Section S.3 in the supplementary materials; the left plot of panel (b) shows posterior probabilities $p(\text{HR} < 0.6 | \text{Data})$ under repeat simulations, and on the right posterior estimated hazard ratios for OS with pointwise 95% credible regions are shown, under H_0 (blue) and H_1 (red).

the posterior probability $p_\ell \equiv p(\text{HR} < 0.6 | \text{Data})$ (with ℓ indexing the $L = 100$ repeat simulations) at time horizon 50 weeks under the proposed model. The left panel of Figure 6(b) shows histograms of p_ℓ under H_0 (in blue) and under H_1 (in red). As desired, under H_0 , the posterior probabilities are clustered close to zero, whereas under H_1 the histogram is sharply peaked close to 1.0.

Finally, we again identify a representative simulation by selecting the repeat simu-

lation ℓ with posterior probability p_ℓ closest to the median of the respective histograms under each of the two scenarios. For each of the two scenarios, we plot the posterior estimated hazard ratios (blue and red for simulation under H_0 and H_1 , respectively), together with pointwise 95% posterior credible intervals in the right panel of Figure 6(b). Under H_0 (blue), HR is almost equal to 1 with wide credible intervals, whereas under H_1 (red), HR is significantly below 1 with high posterior probability. The median (over the L simulations) posterior probabilities $p_{\hat{\ell}}(\text{HR} < 0.6 \mid \text{Data})$ are 0.08 and 0.98 under H_0 and H_1 , respectively.

8 Discussion

With a long term objective of setting up a platform for future single-arm early-phase clinical trials in GBM, where new patients only receive experimental therapies, in this article, we developed a Bayesian nonparametric approach for creating synthetic controls from RWD. We introduce a Bayesian common atoms mixture (CAM) model that clusters covariates with similar values across different treatment arms.

The flexibility of the CAM model makes it easily generalizable to other problems, for example, to create two synthetic treatment arms to compare two treatments based on RWD from electronic health records.

Another direction of extensions could build on extracting propensity scores as inference summaries under the CA-PPMx model. This is briefly discussed in Section S.4 of the supplementary materials.

A limitation of the current model is scalability to high-dimensional covariates. In the GBM application, we take into account 11 clinically important categorical covariates commonly considered as prognostic factors in GBM treatments. However, in many applications covariates can be quite high-dimensional and Bayesian mixture

models suffer from the curse of dimensionality. Implicit in the current construction is the assumption that the recorded covariates are clinically relevant for the disease or condition under consideration and the approach may not be appropriate when large numbers of unscreened candidate covariates are used. Recent advances in Bayesian model-based clustering by [Chandra *et al.* \(2021\)](#) could be useful to construct high-dimensional generalizations.

Supplementary Materials

Supplementary materials include additional discussion on the motivating dataset, a brief review on the PPMx, detailed discussion on the graphical goodness-of-fit test of our regression model, an alternative interpretation of our model-based inference approach, choice of hyperparameters and detailed posterior simulation scheme.

References

- Aldape, K., Brindle, K. M., *et al.* (2019). Challenges to curing primary brain tumours. *Nature Reviews Clinical Oncology*, **16**, 509–520.
- Alexander, B. M., Trippa, L., Gaffey, S., *et al.* (2019). Individualized screening trial of innovative Glioblastoma therapy (INSIGHt): A Bayesian adaptive platform trial to develop precision medicines for patients with Glioblastoma. *JCO Precision Oncology*, **3**, 1–13.
- Au, S. and Beck, J. (2003). Important sampling in high dimensions. *Structural Safety*, **25**, 139–163.
- Baker, S. G. and Lindeman, K. S. (2001). Rethinking historical controls. *Biostatistics*, **2**, 383–396.
- Berry, S. M., Carlin, B. P., Lee, J. J., and Müller, P. (2010). *Bayesian adaptive methods for clinical trials*. CRC Press.
- Breiman, L. (2001). Random forests. *Machine Learning*, **45**, 5–32.
- Burcu, M., Dreyer, N. A., *et al.* (2020). Real-world evidence to support regulatory decision-making for medicines: Considerations for external control arms. *Pharmacoepidemiology and Drug Safety*, **29**, 1228–1235.
- Camerlenghi, F., Dunson, D. B., Lijoi, A., Prünster, I., and Rodríguez, A. (2019). Latent nested nonparametric priors (with discussion). *Bayesian Analysis*, **14**, 1303–1356.

- Chandra, N. K., Canale, A., and Dunson, D. B. (2021). Escaping the curse of dimensionality in Bayesian model-based clustering. *arXiv preprint arXiv:2006.02700*.
- Chen, M.-H. and Ibrahim, J. G. (2000). Power prior distributions for regression models. *Statistical Science*, **15**, 46–60.
- Chen, W.-C., Wang, C., Li, H., Lu, N., Tiwari, R., Xu, Y., and Yue, L. Q. (2020). Propensity score-integrated composite likelihood approach for augmenting the control arm of a randomized controlled trial by incorporating real-world data. *Journal of Biopharmaceutical Statistics*, **30**, 508–520.
- Chipman, H. A., George, E. I., and McCulloch, R. E. (2010). BART: Bayesian additive regression trees. *Annals of Applied Statistics*, **4**, 266–298.
- Choi, J., Dekkers, O. M., and le Cessie, S. (2019). A comparison of different methods to handle missing data in the context of propensity score analysis. *European Journal of Epidemiology*, **34**, 23–36.
- Cox, D. R. (1972). Regression models and life-tables. *Journal of the Royal Statistical Society. Series B (Methodological)*, **34**, 187–220.
- Dahl, D. B. (2006). *Model-based clustering for expression data via a Dirichlet process mixture model*, pages 201–218. Cambridge University Press.
- Davi, R., Mahendraratnam, N., Chatterjee, A., *et al.* (2020). Informing single-arm clinical trials with external controls. *Nature Reviews Drug Discovery*, **19**, 821–822.
- Denti, F., Camerlenghi, F., Guindani, M., and Mira, A. (2021). A common atoms model for the Bayesian nonparametric analysis of nested data. *Journal of the American Statistical Association*. To appear.
- FDA (2020). Rare diseases at FDA. <https://www.fda.gov/patients/rare-diseases-fda>. Accessed on 7th Dec, 2021.
- FDA (2021). *Adjusting for Covariates in Randomized Clinical Trials for Drugs and Biological Products*. Guidance for Industry, <https://www.fda.gov/regulatory-information/search-fda-guidance-documents/adjusting-covariates-randomized-clinical-trials-drugs-and-biological-products>.
- Ferguson, T. S. (1973). A Bayesian analysis of some nonparametric problems. *Annals of Statistics*, **1**, 209–230.
- Fisher, J. P. and Adamson, D. C. (2021). Current FDA-approved therapies for high-grade malignant gliomas. *Biomedicines*, **9**.
- Franklin, J. M., Glynn, R. J., Martin, D., and Schneeweiss, S. (2019). Evaluating the use of nonrandomized real-world data analyses for regulatory decision making. *Clinical Pharmacology & Therapeutics*, **105**, 867–877.
- Ghosal, S., Ghosh, J. K., and Ramamoorthi, R. V. (1999). Posterior consistency of Dirichlet mixtures in density estimation. *Annals of Statistics*, **27**, 143–158.

- Green, P. J. (1995). Reversible jump Markov chain Monte Carlo computation and Bayesian model determination. *Biometrika*, **82**, 711–732.
- Grossman, S. A. and Ellsworth, S. G. (2016). Published glioblastoma clinical trials from 1980 to 2013: Lessons from the past and for the future. *Journal of Clinical Oncology*, **34**, e13522–e13522.
- Grossman, S. A., Schreck, K. C., Ballman, K., and Alexander, B. (2017). Point/counterpoint: Randomized versus single-arm phase II clinical trials for patients with newly diagnosed glioblastoma. *Neuro-Oncology*, **19**, 469–474.
- Haase, S., Garcia-Fabiani, M. B., *et al.* (2018). Mutant ATRX: Uncovering a new therapeutic target for glioma. *Expert Opinion on Therapeutic Targets*, **22**, 599–613.
- Hasegawa, T., Claggett, B., *et al.* (2017). The myth of making inferences for an overall treatment efficacy with data from multiple comparative studies via meta-analysis. *Statistics in Biosciences*, **9**, 284–297.
- Hobbs, B. P., Carlin, B. P., Mandrekar, S. J., and Sargent, D. J. (2011). Hierarchical commensurate and power prior models for adaptive incorporation of historical information in clinical trials. *Biometrics*, **67**, 1047–1056.
- Jiang, L., Nie, L., and Yuan, Y. (2021). Elastic priors to dynamically borrow information from historical data in clinical trials. *Biometrics*. (To appear).
- Johnson, V. E. (2007). Bayesian model assessment using pivotal quantities. *Bayesian Analysis*, **2**, 719–733.
- King, G. and Nielsen, R. (2019). Why propensity scores should not be used for matching. *Political Analysis*, **27**, 435–454.
- Li, X. and Song, Y. (2020). Target population statistical inference with data integration across multiple sources-an approach to mitigate information shortage in rare disease clinical trials. *Statistics in Biopharmaceutical Research*, **12**, 322–333.
- Lu, N., Wang, C., *et al.* (2021). Leverage multiple real-world data sources in single-arm medical device clinical studies. *Journal of Biopharmaceutical Statistics*. To appear.
- Mandel, J. J., Yust-Katz, S., *et al.* (2017). Inability of positive phase II clinical trials of investigational treatments to subsequently predict positive phase III clinical trials in glioblastoma. *Neuro-Oncology*, **20**, 113–122.
- Meloun, M. and Militký, J. (2011). The exploratory and confirmatory analysis of univariate data. In *Statistical Data Analysis*, pages 25–71. Woodhead Publishing India.
- Müller, P., Quintana, F., and Rosner, G. L. (2011). A product partition model with regression on covariates. *Journal of Computational and Graphical Statistics*, **20**, 260–278.

- Nam, J. Y. and de Groot, J. F. (2017). Treatment of glioblastoma. *Journal of Oncology Practice*, **13**, 629–638.
- Nichol, A., Bailey, M., and Cooper, D. (2010). Challenging issues in randomised controlled trials. *Injury*, **41**, S20–S23.
- Ostrom, Q. T., Gittleman, H., *et al.* (2016). CBTRUS statistical report: Primary brain and other central nervous system tumors diagnosed in the United States in 2009–2013. *Neuro-Oncology*, **18**, v1–v75.
- Page, G. L., Quintana, F. A., and Müller, P. (2021). Clustering and prediction with variable dimension covariates. *Journal of Computational and Graphical Statistics*. (To appear).
- Patel, B. and Kim, A. H. (2020). Laser interstitial thermal therapy. *Missouri Medicine*, **117**, 50–55.
- Peto, R. and Peto, J. (1972). Asymptotically efficient rank invariant test procedures. *Journal of the Royal Statistical Society. Series A (General)*, **135**, 185–207.
- Prevost, T. C., Abrams, K. R., and Jones, D. R. (2000). Hierarchical models in generalized synthesis of evidence: An example based on studies of breast cancer screening. *Statistics in Medicine*, **19**, 3359–3376.
- Rodríguez, A., Dunson, D. B., and Gelfand, A. E. (2008). The nested Dirichlet process. *Journal of the American Statistical Association*, **103**, 1131–1154.
- Rosenbaum, P. R. and Rubin, D. B. (1983). The central role of the propensity score in observational studies for causal effects. *Biometrika*, **70**, 41–55.
- Schmidli, H., Häring, D. A., Thomas, M., Cassidy, A., Weber, S., and Bretz, F. (2020). Beyond randomized clinical trials: Use of external controls. *Clinical Pharmacology & Therapeutics*, **107**, 806–816.
- Sethuraman, J. (1994). A constructive definition of Dirichlet priors. *Statistica Sinica*, **4**, 639–650.
- Skare, O., Bølviken, E., and Holden, L. (2003). Improved sampling-importance resampling and reduced bias importance sampling. *Scandinavian Journal of Statistics*, **30**, 719–737.
- Stuart, E. A. (2010). Matching methods for causal inference: A review and a look forward. *Statistical Science*, **25**, 1–21.
- Sutton, A. J. and Abrams, K. R. (2001). Bayesian methods in meta-analysis and evidence synthesis. *Statistical Methods in Medical Research*, **10**, 277–303.
- Teh, Y. W., Jordan, M. I., Beal, M. J., and Blei, D. M. (2006). Hierarchical Dirichlet processes. *Journal of the American Statistical Association*, **101**, 1566–1581.

- Vanderbeek, A. M., Rahman, R., Fell, G., Ventz, S., Chen, T., Redd, R., Parmigiani, G., Cloughesy, T. F., Wen, P. Y., Trippa, L., and Alexander, B. M. (2018). The clinical trials landscape for glioblastoma: Is it adequate to develop new treatments? *Neuro-Oncology*, **20**, 1034–1043.
- Vansteelandt, S. and Daniel, R. (2014). On regression adjustment for the propensity score. *Statistics in Medicine*, **33**, 4053–4072.
- Ventz, S., Lai, A., Cloughesy, T. F., Wen, P. Y., Trippa, L., and Alexander, B. M. (2019). Design and evaluation of an external control arm using prior clinical trials and real-world data. *Clinical Cancer Research*, **25**, 4993–5001.
- Wang, C. and Rosner, G. L. (2019). A Bayesian nonparametric causal inference model for synthesizing randomized clinical trial and real-world evidence. *Statistics in Medicine*, **38**, 2573–2588.
- Wang, C., Li, H., Chen, W.-C., *et al.* (2019). Propensity score-integrated power prior approach for incorporating real-world evidence in single-arm clinical studies. *Journal of Biopharmaceutical Statistics*, **29**, 731–748.
- Zhao, Z. (2004). Using matching to estimate treatment effects: Data requirements, matching metrics, and Monte Carlo evidence. *The Review of Economics and Statistics*, **86**, 91–107.

Supplementary Materials for Bayesian Nonparametric Common Atoms Regression for Generating Synthetic Controls in Clinical Trials

Noirrit Kiran Chandra^a (noirritchandra@utexas.edu)

Abhra Sarkar^a (abhra.sarkar@utexas.edu)

John F. de Groot^b (john.degroot@ucsf.edu)

Ying Yuan^c (yyuan@mdanderson.org)

Peter Müller^{a,d} (pmueller@math.utexas.edu)

^aDepartment of Statistics and Data Sciences,
The University of Texas at Austin, TX, USA

^bDepartment of Neurological Surgery,
University of California San Francisco, CA, USA

^cDepartment of Biostatistics,
The University of Texas MD Anderson Cancer Center, Houston, TX, USA

^dDepartment of Mathematics,
The University of Texas at Austin, TX, USA

Supplementary materials present additional discussion on the motivating dataset, a brief review on the PPMx, detailed discussion on the graphical goodness-of-fit test of our regression model, an alternative interpretation of our model-based inference approach, choice of hyperparameters and detailed posterior simulation scheme.

S.1 Historical Data and Potential Future Trial

Figure S.1 shows summaries for the covariates described in Section 2 in the historical database and a potential future single-arm trial. Marginal frequencies for each of the covariates are plotted clearly highlighting the differences between the two populations.

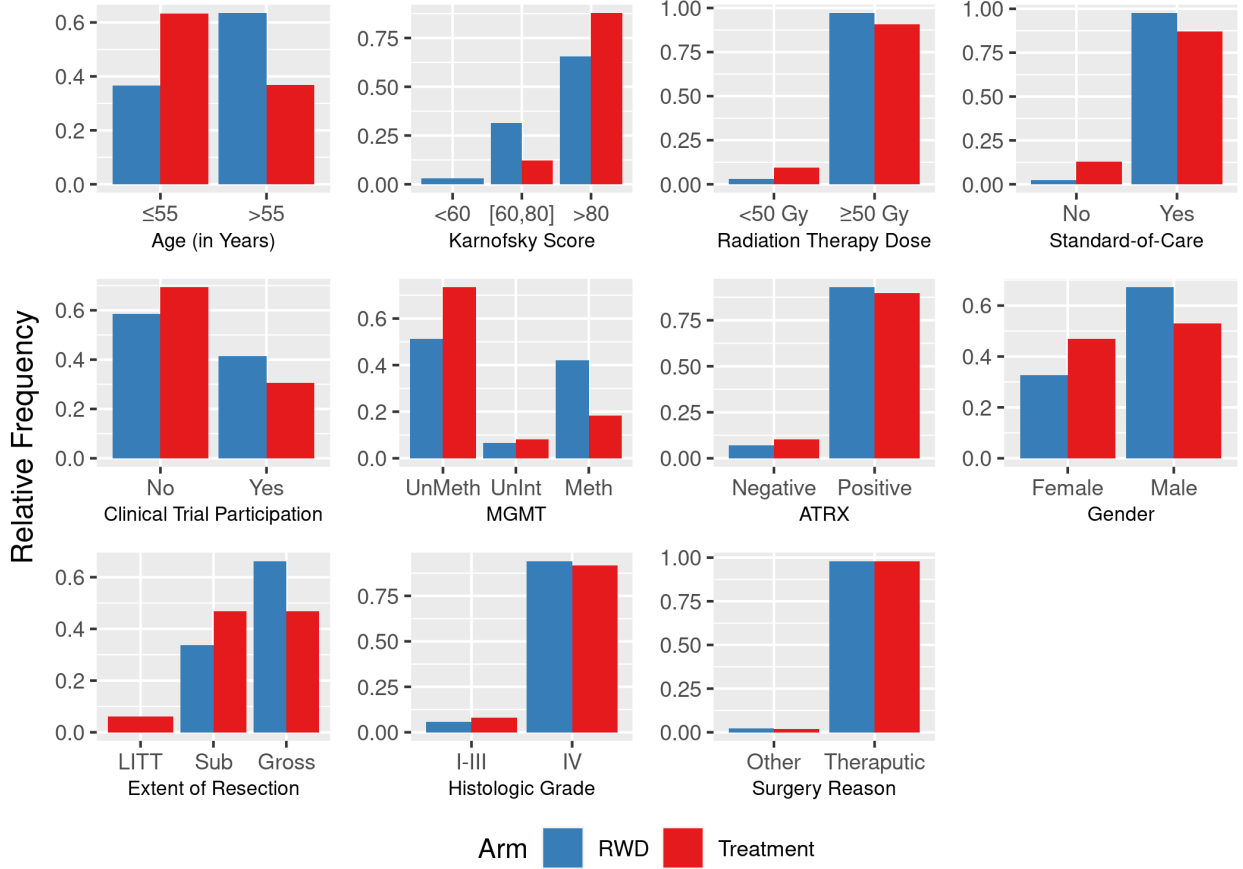


Figure S.1: Relative frequency plots of the covariates in the two treatment arms.

S.2 Product Partition Model with Regression (PPMx)

Let $i = 1, \dots, n$ be the indices of n data points and for the i^{th} unit, the data consists of covariates $\mathbf{X}_i = (X_{i,1}, \dots, X_{i,p})^T$ and response variables \mathbf{Y}_i . Let $\mathbf{X} = \{\mathbf{X}_1, \dots, \mathbf{X}_n\}$ and $\mathbf{Y} = \{\mathbf{Y}_1, \dots, \mathbf{Y}_n\}$ be the complete set of covariates and responses respectively. Let $\boldsymbol{\rho}_n = \{S_1, \dots, S_{k_n}\}$ denote a partition of the n units into k_n subsets, where $1 \leq k_n \leq n$. An equivalent representation of $\boldsymbol{\rho}_n$ introduces cluster membership indicators $c_i = j$ if and only if $i \in S_j$. Let \mathbf{X}_j be the covariates corresponding to the samples in S_j . In the PPMx, it is believed that data points with very similar covariate values are more likely to *a priori* be in the same cluster and the corresponding responses are also very similar. The prior consists of

two functions - (i) a cohesion function denoted by $c(S_j | \alpha) \geq 0$ for $S_j \subset \{1, \dots, n\}$ associated with a hyper-parameter α discerning the prior belief of co-clustering of the elements of S_j , and (ii) a similarity function denoted by $\mathbf{g}(\mathbf{X}_j | \boldsymbol{\xi})$ and parametrized by $\boldsymbol{\xi}$, formalizing the ‘closeness’ of the \mathbf{X}_i ’s in the cluster S_j by producing larger values of $\mathbf{g}(\mathbf{X}_j | \boldsymbol{\xi})$ for \mathbf{X}_i ’s that are more similar. With the similarity and cohesion functions, the form of the PPMx prior is the following product

$$\Pi(\boldsymbol{\rho}_n | \mathbf{X}, \alpha, \boldsymbol{\xi}) \propto \prod_{j=1}^{k_n} c(S_j | \alpha) \mathbf{g}(\mathbf{X}_j | \boldsymbol{\xi}). \quad (\text{S.1})$$

Page *et al.* (2021) considered $c(S_j | \alpha) = \alpha \times (|S_j| - 1)!$, where $\alpha > 0$ and $|\cdot|$ being the cardinality of a set, which is identical to the induced prior on the partitions in a Chinese restaurant process (Ferguson, 1973). Müller *et al.* (2011) suggested the following similarity function

$$\mathbf{g}(\mathbf{X}_j | \boldsymbol{\xi}) = \int \prod_{i \in S_j} \mathbf{q}(\mathbf{X}_i | \boldsymbol{\zeta}_j) \bar{\mathbf{q}}(\boldsymbol{\zeta}_j | \boldsymbol{\xi}) d\boldsymbol{\zeta}_j. \quad (\text{S.2})$$

With a conjugate sampling model and prior pair of \mathbf{q} and $\bar{\mathbf{q}}$, the integral in (S.2) is analytically available, facilitating easy computation. The pair is used to assess the agreement of the data points in S_j rather than any notion of statistical modeling.

The model construction is concluded by specifying a sampling model for the response variable \mathbf{Y}_i ’s. With the assertion that responses corresponding to similar valued covariates are also similar (which is satisfied for the linear regression), sampling models for each cluster of similar-valued covariates can be defined. In other words, a mixture model is assumed on the response variables, where the partition of the mixture distribution is induced by the covariates. For a given partition $\boldsymbol{\rho}_n$, with the introduction of cluster specific parameters $\boldsymbol{\theta} = \{\boldsymbol{\theta}_1, \dots, \boldsymbol{\theta}_{k_n}\}$, the model can be expressed hierarchically as:

$$\mathbf{Y}_i | \boldsymbol{\theta}, c_i = j \stackrel{\text{ind}}{\sim} h(\mathbf{Y}_i | \boldsymbol{\theta}_j), \quad \boldsymbol{\theta}_j | \boldsymbol{\varphi} \stackrel{\text{iid}}{\sim} \Pi(\boldsymbol{\theta}_j | \boldsymbol{\varphi}), \quad (\text{S.3})$$

where h is a sampling model and $\Pi(\cdot | \boldsymbol{\varphi})$ is the prior on $\boldsymbol{\theta}_j$ with hyper-parameter $\boldsymbol{\varphi}$.

Even though \mathbf{X}_i ’s may not be random, with slight abuse of notations, one may equivalently express the PPMx as the following mixture model

$$\mathbf{X}_i | c_i = j, \boldsymbol{\zeta} \stackrel{\text{iid}}{\sim} \mathbf{q}(\mathbf{X}_i | \boldsymbol{\zeta}_j), \quad \boldsymbol{\zeta}_j | \boldsymbol{\xi} \stackrel{\text{iid}}{\sim} \bar{\mathbf{q}}(\boldsymbol{\zeta}_j | \boldsymbol{\xi}), \quad c_i \stackrel{\text{iid}}{\sim} \text{Mult}(\boldsymbol{\pi}), \quad \boldsymbol{\pi} \sim \Pi_\pi, \quad (\text{S.4})$$

where $\boldsymbol{\zeta} = \{\boldsymbol{\zeta}_j\}_{j=1}^\infty$ can be considered as the atoms of the mixture model, $\boldsymbol{\pi}$ is the vector of weights attached to the atoms, and Π_π is the prior on the mixture weights induced from the chosen cohesion function. For $c(S_j | \alpha) = \alpha \times (|S_j| - 1)!$, Π_π is the stick-breaking prior $\text{GEM}(\alpha)$ on mixture weights derived from a DP with mass parameter α (Sethuraman, 1994). The number of mixture components can be infinity for a variety of other stick-breaking type priors (Pitman, 1996) as well.

S.3 Goodness-of-Fit Test for Continuous Responses

We generalize the results of [Johnson \(2007\)](#) to derive a graphical goodness-of-fit tool to validate the mixture of lognormal model for the CA-PPMx. The procedure is valid as long as h in (6) is a univariate continuous density, i.e., as long as the response variables are univariate and continuous. For the moment we suppress the additional s subindex on (\mathbf{X}_i, Y_i) , $i = 1, \dots, n$. Let $m(\mathbf{Y} \mid \mathbf{X})$ be the marginal distribution after integrating out all model parameters

$$m(\mathbf{Y} \mid \mathbf{X}) = \sum_{\mathbf{c}} \int \left\{ \prod_{i=1}^n h(Y_i \mid \boldsymbol{\theta}_{c_i}) \right\} dp(\boldsymbol{\theta}, \mathbf{c}_{1:n} \mid \mathbf{X}).$$

We implement a test of fit based on the following result. Assuming that $m(\mathbf{Y} \mid \mathbf{X})$ is the true marginal distribution of \mathbf{Y} , we have:

Proposition 1. *Let $\boldsymbol{\omega} = (\boldsymbol{\theta}, \mathbf{c}_{1:n})$ be a sample from their posterior, $H(y \mid \boldsymbol{\theta}) = \int_{-\infty}^y h(z \mid \boldsymbol{\theta}) dz$ be the CDF, and $U_i = H(Y_i \mid \boldsymbol{\theta}_{c_i})$, $i = 1, \dots, n$. Then, $U_i \stackrel{iid}{\sim} \text{Unif}(0, 1)$.*

Proof. Let $\mathbf{u}_{1:n} = \{u_1, \dots, u_n\}$ and define the set $A(\mathbf{u}_{1:n}; \boldsymbol{\omega}) = \cap_{i=1}^n \{y : H(y \mid \boldsymbol{\theta}_{c_i}) \leq u_i\}$. Then,

$$\Pr(U_i \leq u_i \text{ for all } i = 1, \dots, n) = \int \int_{A(\mathbf{u}_{1:n}; \boldsymbol{\omega})} d\Pi(\boldsymbol{\omega} \mid \mathbf{X}, \mathbf{Y}) m(\mathbf{Y} \mid \mathbf{X}) d\mathbf{Y}.$$

Note that $\Pi(\boldsymbol{\omega} \mid \mathbf{X}, \mathbf{Y}) = \{\prod_{i=1}^n h(Y_i \mid \boldsymbol{\theta}_{c_i})\} \Pi(\boldsymbol{\omega} \mid \mathbf{X}) / m(\mathbf{Y} \mid \mathbf{X})$. Substituting this in the above equation, we get

$$\Pr(U_i \leq u_i \text{ for all } i = 1, \dots, n) = \int \left\{ \int_{A(\mathbf{u}_{1:n}; \boldsymbol{\omega})} \prod_{i=1}^n h(Y_i \mid \boldsymbol{\theta}_{c_i}) d\mathbf{Y} \right\} d\Pi(\boldsymbol{\omega} \mid \mathbf{X}).$$

Now, the term inside the parenthesis integrates to $\prod_{i=1}^n u_i$ which is independent from $\Pi(\boldsymbol{\omega} \mid \mathbf{X})$. Hence the proof. \square

To understand the implications, consider the joint distribution of $(\mathbf{Y}, \boldsymbol{\omega})$ given \mathbf{X} . Then first sample $\tilde{\boldsymbol{\omega}} = (\tilde{\boldsymbol{\theta}}, \tilde{\mathbf{c}}_{1:n})$ from $p(\boldsymbol{\omega} \mid \mathbf{X}) = p(\mathbf{c} \mid \mathbf{X}) p(\boldsymbol{\theta} \mid \mathbf{c}, \mathbf{X})$ and then $(\mathbf{Y} \mid \tilde{\boldsymbol{\omega}}, \mathbf{X})$ from the sampling model (6). Letting $\tilde{U}_i = H(Y_i \mid \tilde{\boldsymbol{\theta}}_{\tilde{c}_i})$, we then have $\tilde{U}_i \stackrel{iid}{\sim} \text{Unif}(0, 1)$. Assuming that the observed data \mathbf{Y} does in fact arise from the assumed marginal model $m(\mathbf{Y} \mid \mathbf{X})$, Proposition 1 sets up sampling from the alternative factorization $p(\mathbf{Y}, \boldsymbol{\omega} \mid \mathbf{X}) = m(\mathbf{Y} \mid \mathbf{X}) \cdot p(\boldsymbol{\omega} \mid \mathbf{Y}, \mathbf{X})$. It follows that $\tilde{\mathbf{U}}_{1:n}$ and $\mathbf{U}_{1:n}$ are indistinguishable in distribution. The latter, $\mathbf{U}_{1:n}$ can be readily obtained from the posterior samples of $\boldsymbol{\omega}$. Letting $\mathbf{U}_{1:n}^{(m)}$ denote the evaluation under the m^{th} posterior MCMC sample $\boldsymbol{\omega}^{(m)}$, a goodness-of-fit test can then be carried out to validate the uniform distribution.

Note that the $\mathbf{U}_{1:n}^{(m)}$'s vary across different posterior samples $\boldsymbol{\omega}^{(m)}$ while also having hierarchical dependence since all of them are sampled conditionally on the same \mathbf{Y} (and \mathbf{X}). Although in principle formal prior-predictive-posterior based tests be carried out ([Johnson, 2007](#); [Cao et al., 2010](#)), it can be numerically infeasible for complex models like ours. As a practical alternative, goodness-of-fit can be assessed from visual inspections of the quantile-quantile plots of $\mathbf{U}_{1:n}^{(m)}$. Such visual tools can be effective for detecting departures from model

assumptions (Meloun and Miltký, 2011, Chapter 2) and we use it to assess the model fit in Section 7.

To assess the goodness-of-fit in the GBM application, where the outcomes are right-censored survival data, we extend the result in the following corollary.

Corollary 1. *Suppose we have right-censored survival outcomes (Y_i, ν_i) with covariate \mathbf{X}_i where $\nu_i = 1$ if Y_i is an observed failure time, for $i = 1, \dots, n$. Following the notations of Theorem 1, define $U_i = H(Y_i | \boldsymbol{\theta}_{c_i})$ if $\nu_i = 1$, else if $\nu_i = 0$ define $U_i = H(Y_i | \boldsymbol{\theta}_{c_i}) + \gamma_i \{1 - H(Y_i | \boldsymbol{\theta}_{c_i})\}$, where $\gamma_i \stackrel{iid}{\sim} \text{Unif}(0, 1)$ independent from Y_i . If the observed failure times are independent of the censoring times, then $U_i \stackrel{iid}{\sim} \text{Unif}(0, 1)$.*

Proof of Corollary 1. Let \tilde{Y}_i be the true failure time of the i^{th} individual, that is $\tilde{Y}_i \geq Y_i$ with equality if and only if $\nu_i = 1$. Letting $\tilde{U}_i = H(\tilde{Y}_i | \boldsymbol{\theta}_{c_i})$, Theorem 1 implies $\tilde{U}_{1:n} \stackrel{iid}{\sim} \text{Unif}(0, 1)$. Note that

$$H(\tilde{Y}_i | \boldsymbol{\theta}_{c_i}) = \nu_i H(\tilde{Y}_i | \boldsymbol{\theta}_{c_i}) + (1 - \nu_i) \left[H(Y_i | \boldsymbol{\theta}_{c_i}) + \{H(\tilde{Y}_i | \boldsymbol{\theta}_{c_i}) - H(Y_i | \boldsymbol{\theta}_{c_i})\} \right].$$

Since, $H(\tilde{Y}_i | \boldsymbol{\theta}_{c_i}) \sim \text{Unif}(0, 1)$ and is independent of Y_i , $H(Y_i | \boldsymbol{\theta}_{c_i}) + \{H(\tilde{Y}_i | \boldsymbol{\theta}_{c_i}) - H(Y_i | \boldsymbol{\theta}_{c_i})\} | Y_i, \boldsymbol{\theta}_{c_i} \sim \text{Unif}\{H(Y_i | \boldsymbol{\theta}_{c_i}), 1\}$ which follows the same distribution as $\gamma_i \{1 - H(Y_i | \boldsymbol{\theta}_{c_i})\}$. Hence the proof. \square

S.4 Alternate Interpretation of the CA-PPMx

In Section 4.2 we introduced a model-based approach for inference on treatment effects in the CA-PPMx model. Yet another alternative interpretation of the same approach arises from observing the following connection with methods based on PS stratification (Wang et al., 2019; Chen et al., 2020; Lu et al., 2021). The CAM model can be interpreted as a stochastic PS stratification. To see this, first re-index all patients and patient specific variables across $s = 1, 2$ as $i = 1, \dots, N = n_1 + n_2$ and define $Z_i \in \{1, 2\}$ if patient i was originally in data set $s = 1$ or 2 , respectively. For the sake of brevity assuming equal sample sizes $n_1 = n_2$, we have $p(Z_i = 1 | c_i = j) / p(Z_i = 2 | c_i = j) = \pi_{1,j} / \pi_{2,j}$. That is, the terms in the CAM model correspond to different PS ratios for the selection of a patient into $s = 1$ versus $s = 2$. Grouping patients in clusters C_j is then interpreted as stratification by PS, with clusters C_j defining the strata. Within each stratum we report treatment effect $\delta_j = \delta\{h(Y | \boldsymbol{\theta}_{1,j}), h(Y | \boldsymbol{\theta}_{2,j})\}$. If δ were just a difference of means, and $\boldsymbol{\theta}$ were to represent the mean of $h(\cdot | \boldsymbol{\theta})$, the latter might simplify to $\delta_j = \boldsymbol{\theta}_{1,j} - \boldsymbol{\theta}_{2,j}$. Averaging and taking posterior expectations this motivates again to report $\tilde{\Delta}_\theta = \sum \pi_{1,j} [\mathbb{E}_{h(Y|\boldsymbol{\theta}_{1,j})}\{T(Y)\} - \mathbb{E}_{h(Y|\boldsymbol{\theta}_{2,j})}\{T(Y)\}] = \sum \pi_{1,j} (\boldsymbol{\theta}_{1,j} - \boldsymbol{\theta}_{2,j})$. Whereas fixed consolidated unidimensional PSs may be inadequate in matching multivariate covariates (Stuart, 2010; King and Nielsen, 2019) and hence sensitive to the specification of the PS model (Zhao, 2004), inference under the proposed CAM model overcomes limitations by naturally including uncertainty on the stratification in the inference.

S.5 Model Specifications and Hyperparameters

Recall the setup from Section 3.1 and the notations from eqn (4). for categorical covariate $X_{s,\ell}$ with categories $1, \dots, m_\ell$, we choose $q_\ell(X_{s,\ell} \mid \boldsymbol{\zeta}_\ell) = \text{Mult}(1; \zeta_{\ell,1}, \dots, \zeta_{\ell,m_\ell})$ and $\bar{q}(\zeta_{\ell,1}, \dots, \zeta_{\ell,m_\ell}) = \text{Dir}(1, \dots, 1)$. For continuous $X_{s,\ell}$, we choose $q_\ell(X_{s,\ell} \mid \boldsymbol{\zeta}_\ell) = \text{N}(X_{s,\ell}; \mu_{X,\ell}, \sigma_{X,\ell}^2)$ with $\boldsymbol{\zeta}_\ell = (\mu_{X,\ell}, \sigma_{X,\ell}^2)$ and $\bar{q}(\mu_{X,\ell}, \sigma_{X,\ell}^2) = \text{NIG}(\mu_{X,\ell}, \sigma_{X,\ell}^2; 0, 1, \alpha_X, 1)$, i.e., $\mu_{X,\ell} \mid \sigma_{X,\ell}^2 \sim \text{N}(0, \sigma_{X,\ell}^2)$, $\sigma_{X,\ell}^{-2} \sim \text{Ga}(a_X, 1)$. We set $a_X = \#\text{continuous covariates} + 30$. As regarding the hyperparameters concerning the cluster weights in models (1) and (3), we choose $\alpha_1 = \alpha_2 = 1$.

Regarding the parameters of the sampling model for survival outcomes in eqn (8), we set $\kappa_0 = 1$ and $a_0 = 2.1$. Regarding the hyperprior on μ_0 and b_0 , we choose the hyperparameters using an empirical Bayes type approach.

Regarding the real-valued continuous responses in the simulation studies in Section 6, we use the model in eqn (8) on the actual response variables.

S.6 Posterior Computation

For computational convenience in the practical implementation, we consider the *degree k weak limit approximation* (Ishwaran and Zarepour, 2002a,b) of the $\text{GEM}(\alpha_2)$ distribution in (1), that is we consider a $\text{Dir}(\alpha_2/k, \dots, \alpha_2/k)$ distribution instead, for a fixed but large enough k .

We develop a Gibbs sampling algorithm to circumvent the computational issues with a Gaussian mixture models on the log transformed survival outcomes with censoring. Without loss of generality we assume $Y_{s,i}$'s (log transformed outcomes) are supported on the entire real line and describe our algorithm for a mixture of Gaussian distributions on them. Let $\nu_{s,i}$'s be the censoring indicators such that $\nu_{s,i} = 1$ implies $Y_{s,i}$ is an observed failure time; else if it is censored in the interval $(Y_{s,i,l}, Y_{s,i,u})$ then $\nu_{s,i} = 0$. For left and right censoring we take $Y_{s,i,u} = \infty$ and $Y_{s,i,l} = -\infty$ respectively. Let $\tilde{Y}_{s,i}$ be the true failure times, that is $\tilde{Y}_{s,i} = Y_{s,i}$ if and only if $\nu_{s,i} = 1$. Before the MCMC, we initialize $\tilde{Y}_{s,i}$ at some admissible value for $\nu_{s,i} = 0$ and cluster membership indicator variables \mathbf{c}_1 and \mathbf{c}_2 . For the CAM model on covariates, we consider a conjugate sampling and prior pair q_ℓ and \bar{q}_ℓ respectively for the ℓ^{th} covariate for all $\ell = 1, \dots, p$ since this allows to analytically integrate out the atoms $\boldsymbol{\zeta}_j$'s. This strategy results in huge reduction in the number of effective parameters required to be sampled in the MCMC along with substantial improvements in the mixing and numerical efficiency.

The sampler iterates through the following steps. In Step 1, we impute the $\tilde{Y}_{s,i}$'s for the censored observations which allows to take the computational advantages of a Gaussian mixture model; in Step 2, we update the cluster membership indicators \mathbf{c}_1 and \mathbf{c}_2 ; in Step 3, we update hyper-parameters related to the response model that allows sharing of information via a hierarchical model; and in Step 4, we update the parameters required to implement

the strategies outlined in Sections 3.2 and 4.2.

Step 1 We define the set $S_{s,j,-i} = \{i : c_{s,i} = j\} \setminus \{i\}$, $n_{s,j,-i} = |S_{s,j,-i}|$, $\kappa_{s,j,-i} = \kappa_0 + n_{s,j,-i}$, $\bar{Y}_{s,j,-i} = \sum_{r \in S_{s,j,-i}} \tilde{Y}_{s,r} / n_{s,j,-i}$, $\mu_{s,j,-i} = (\kappa_0 \mu_0 + n_{s,j,-i} \bar{Y}_{s,j,-i}) / \kappa_{s,j,-i}$, $a_{s,j,-i} = a_0 + n_{s,j,-i} / 2$, $b_{s,j,-i} = b_0 + \sum_{r \in S_{s,j,-i}} (\tilde{Y}_{s,r} - \bar{Y}_{s,j,-i})^2 / 2 + n_{s,j,-i} \kappa_0 (\bar{Y}_{s,j,-i} - \mu_0)^2 / \kappa_{s,j,-i}$. Then for all $i = 1, \dots, n_s$ and $s = 1, 2$, generate

$$\tilde{Y}_{s,i} \sim \begin{cases} Y_{s,i} \text{ with probability 1 if } \nu_{s,i} = 1; \\ t_{2a_{s,j,-i}} \left\{ \mu_{s,j,-i}, \frac{b_{s,j,-i}(\kappa_{s,j,-i}+1)}{a_{s,j,-i}\kappa_{s,j,-i}} \mid (Y_{s,i,l}, Y_{s,i,u}) \right\}, \end{cases}$$

where $t_q\{\mu, \sigma^2 \mid (a, b)\}$ is a central Student's t -distribution, with degrees of freedom q , median μ and scale paramter σ , truncated to the set (a, b) .

Step 2 Letting $f_t\{\cdot \mid q, \mu, \sigma^2\}$ and $F_t\{\cdot \mid q, \mu, \sigma^2\}$ denote the pdf and cdf of a central Student's t -distribution with degrees of freedom q , median μ and scale parameter σ respectively, we define

$$\psi_{Y;s,j}(i) = \begin{cases} f_t \left\{ Y_{s,i} \mid 2a_{s,j,-i}, \mu_{s,j,-i}, \frac{b_{s,j,-i}(\kappa_{s,j,-i}+1)}{a_{s,j,-i}\kappa_{s,j,-i}} \right\} & \text{if } \nu_{s,i} = 1; \\ F_t \left\{ Y_{s,i,u} \mid 2a_{s,j,-i}, \mu_{s,j,-i}, \frac{b_{s,j,-i}(\kappa_{s,j,-i}+1)}{a_{s,j,-i}\kappa_{s,j,-i}} \right\} \\ - F_t \left\{ Y_{s,i,l} \mid 2a_{s,j,-i}, \mu_{s,j,-i}, \frac{b_{s,j,-i}(\kappa_{s,j,-i}+1)}{a_{s,j,-i}\kappa_{s,j,-i}} \right\} & \text{otherwise.} \end{cases}$$

Recall from Section 3.1 (see page 11) that $\mathcal{O}_{s,i}$ is the set of indices of the covariates observed for $\mathbf{X}_{s,i}$, and define the sets $\mathcal{C}_{j,\ell} = \cup_{s=1}^2 \{i : i \in S_j, \ell \in \mathcal{O}_{s,i}\}$ and $\mathbf{X}_{j,\ell}^{*o} = \cup_{s=1}^2 \{X_{s,i,j} : i \in \mathcal{C}_{j,\ell}\}$. Define the functions $g_\ell(\mathbf{X}_{j,\ell}^{*o} \mid \boldsymbol{\xi}_\ell) = \int \prod_{i \in \mathcal{C}_{j,\ell}} q_\ell(X_{s,i,\ell} \mid \boldsymbol{\zeta}_{j,\ell}) \bar{q}_\ell(\boldsymbol{\zeta}_{j,\ell} \mid \boldsymbol{\xi}_\ell) d\boldsymbol{\zeta}_{j,\ell}$ and $\psi_{X;s,j}(i) = \prod_{\ell \in \mathcal{O}_{s,i}} \frac{g_\ell(\mathbf{X}_{j,\ell}^{*o} \mid \boldsymbol{\xi}_\ell)}{g_\ell[\mathbf{X}_{j,\ell}^{*o} \setminus \{X_{s,i,\ell}\} \mid \boldsymbol{\xi}_\ell]}$. Then, \mathbf{c}_1 can be updated as

$$\Pi(c_{1,i} = j \mid -) \propto (n_{1,j,-i} + \alpha_1 / k_n) \times \psi_{Y;1,j}(i) \times \psi_{X;1,j}(i) \text{ for } j = 1, \dots, k_n.$$

Similarly \mathbf{c}_2 can be updated as

$$\Pi(c_{2,i} = j \mid -) = 1 \text{ if } n_{1,j} > 0 \text{ and } n_{2,j,-i} = 0;$$

else $\Pi(c_{2,i} = j \mid -) \propto (n_{2,j,-i} + \alpha_2 / k) \times \psi_{Y;2,j}(i) \times \psi_{X;2,j}(i) \text{ for } j = 1, \dots, k.$

Step 3 Define $\tilde{b} = \log b_0$ and let $\Pi(\mu_0, \tilde{b} \mid \tilde{\mathbf{Y}}_{1,1:n_1}, \tilde{\mathbf{Y}}_{2,1:n_2})$ be the joint posterior density of μ_0 and \tilde{b} given $\tilde{Y}_{s,i}$'s, $k_{n,1}$ and $k_{n,2}$ be the number of non-empty clusters in the two cohorts respectively. Then,

$$\begin{aligned} \log \Pi(\mu_0, \tilde{b} \mid \tilde{\mathbf{Y}}_{1,1:n_1}, \tilde{\mathbf{Y}}_{2,1:n_2}) = & K - \frac{(\mu_0 - m_\mu)^2}{2s_\mu^2} - \frac{(\tilde{b} - m_b)^2}{2s_b^2} + (k_{n,1} + k_{n,2})a_0\tilde{b} \\ & - \sum_{j=1}^{k_n} \sum_{s=1}^2 \left(a_0 + \frac{n_{s,j}}{2} \right) \log \left[e^{\tilde{b}} + \frac{1}{2} \left\{ \mu_0^2 \kappa_0 + \sum_{i \in S_{s,j}} \tilde{Y}_{s,i}^2 - \frac{(\kappa_0 \mu_0 + n_{s,j} \bar{Y}_{s,j})^2}{\kappa_0 + n_{s,j}} \right\} \right], \end{aligned}$$

where K is a constant and $\bar{Y}_{s,j} = \sum_{i \in S_{s,j}} \tilde{Y}_{s,i}$. We sample μ_0 and \tilde{b} using a Metropolis adjusted Langevin algorithm (Roberts and Tweedie, 1996).

Step 4 For $j = 1, \dots, k$, we define the set $S_{s,j} = \{i : c_{s,i} = j\}$, $\kappa_{s,j} = \kappa_0 + n_{s,j}$, $\mu_{s,j} = (\kappa_0 \mu_0 + n_{s,j} \bar{Y}_{s,j}) / \kappa_{s,j}$, $a_{s,j} = a_0 + n_{s,j} / 2$, $b_{s,j} = b_0 + \sum_{r \in S_{s,j}} (\tilde{Y}_{s,r} - \bar{Y}_{s,j})^2 / 2 + n_{s,j} \kappa_0 (\bar{Y}_{s,j} - \mu_0)^2 / \kappa_{s,j}$. Then

$$\begin{aligned} \mu_{s,j} &\sim t_{2a_{s,j}} \left\{ \mu_{s,j}, \frac{b_{s,j}(\kappa_{s,j} + 1)}{a_{s,j}\kappa_{s,j}} \right\}, & \sigma_{s,j}^{-2} &\sim \text{Ga}(a_{s,j}, b_{s,j}), \\ \boldsymbol{\pi}_1 &\sim \text{Dir} \left(n_{1,1} + \frac{\alpha_1}{k_n}, \dots, n_{1,k_n} + \frac{\alpha_1}{k_n} \right), & \boldsymbol{\pi}_2 &\sim \text{Dir} \left(n_{2,1} + \frac{\alpha_2}{k}, \dots, n_{2,k} + \frac{\alpha_2}{k} \right). \end{aligned} \quad (\text{S.5})$$

For $s = 1$, we only sample for $j = 1, \dots, k_n$ in (S.5). Note that the dimension of $\boldsymbol{\pi}_1$ can vary across MCMC samples.

Remark 1. Note that in Step 2, $\mathcal{C}_{j,\ell}$ is the set of data points in S_j with observed covariate ℓ , $\mathbf{X}_{j,\ell}^{*o}$ is the collection of the observed values of the covariate ℓ in S_j and $g_\ell(\mathbf{X}_{j,\ell}^{*o} \mid \boldsymbol{\xi}_\ell)$ is the joint marginal density of the ℓ^{th} covariate based on $\mathbf{X}_{j,\ell}^{*o}$. A conjugate sampling and prior pair q_ℓ and \bar{q}_ℓ ensures the analytical availability of g_ℓ and $\psi_{X_{s,j}}(i)$ becomes the conditional distribution of $\mathbf{X}_{s,i}$ given $\mathbf{X}_{j,\ell}^{*o}$. For continuous real-valued $X_{s,j,\ell}$, we may take $q_\ell(\cdot \mid \boldsymbol{\zeta}_j)$ to be the univariate Gaussian pdf where $\boldsymbol{\zeta}_j$ is the set of associated mean and variance parameters, and $\bar{q}_\ell(\boldsymbol{\zeta}_j \mid \boldsymbol{\xi}_\ell)$ to be a normal-inverse-gamma density. In this case, the ratio $\frac{g_\ell(\mathbf{X}_{j,\ell}^{*o} \mid \boldsymbol{\xi}_\ell)}{g_\ell[\mathbf{X}_{j,\ell}^{*o} \setminus \{X_{s,j,\ell}\} \mid \boldsymbol{\xi}_\ell]}$ reduces to a central t -distribution density; for categorical $X_{s,j,\ell}$, a convenient choice can be the multinomial-Dirichlet pair which again yields an analytical expression of the ratio.

In the GBM application and simulation studies in Section 6, we have considered conjugate normal-inverse-gamma and multinomial-Dirichlet conjugate pairs for continuous real-valued covariates and categorical covariates respectively.

References

- Cao, J., Moosman, A., and Johnson, V. E. (2010). A Bayesian Chi-squared goodness-of-fit test for censored data models. *Biometrics*, **66**, 426–434.
- Chen, W.-C., Wang, C., Li, H., Lu, N., Tiwari, R., Xu, Y., and Yue, L. Q. (2020). Propensity score-integrated composite likelihood approach for augmenting the control arm of a randomized controlled trial by incorporating real-world data. *Journal of Biopharmaceutical Statistics*, **30**, 508–520.
- Ferguson, T. S. (1973). A Bayesian analysis of some nonparametric problems. *Annals of Statistics*, **1**, 209–230.
- Ishwaran, H. and Zarepour, M. (2002a). Dirichlet prior sieves in finite normal mixtures. *Statistica Sinica*, **12**, 941–963.
- Ishwaran, H. and Zarepour, M. (2002b). Exact and approximate sum representations for the Dirichlet process. *Canadian Journal of Statistics*, **30**, 269–283.

- Johnson, V. E. (2007). Bayesian model assessment using pivotal quantities. *Bayesian Analysis*, **2**, 719–733.
- King, G. and Nielsen, R. (2019). Why propensity scores should not be used for matching. *Political Analysis*, **27**, 435–454.
- Lu, N., Wang, C., *et al.* (2021). Leverage multiple real-world data sources in single-arm medical device clinical studies. *Journal of Biopharmaceutical Statistics*. To appear.
- Meloun, M. and Militký, J. (2011). The exploratory and confirmatory analysis of univariate data. In *Statistical Data Analysis*, pages 25–71. Woodhead Publishing India.
- Müller, P., Quintana, F., and Rosner, G. L. (2011). A product partition model with regression on covariates. *Journal of Computational and Graphical Statistics*, **20**, 260–278.
- Page, G. L., Quintana, F. A., and Müller, P. (2021). Clustering and prediction with variable dimension covariates. *Journal of Computational and Graphical Statistics*. (To appear).
- Pitman, J. (1996). Some developments of the Blackwell-Macqueen urn scheme. *Lecture Notes-Monograph Series*, **30**, 245–267.
- Roberts, G. O. and Tweedie, R. L. (1996). Exponential convergence of Langevin distributions and their discrete approximations. *Bernoulli*, **2**, 341–363.
- Rousseau, J. and Mengersen, K. (2011). Asymptotic behaviour of the posterior distribution in overfitted mixture models. *Journal of the Royal Statistical Society: Series B (Statistical Methodology)*, **73**, 689–710.
- Sethuraman, J. (1994). A constructive definition of Dirichlet priors. *Statistica Sinica*, **4**, 639–650.
- Stuart, E. A. (2010). Matching methods for causal inference: A review and a look forward. *Statistical Science*, **25**, 1–21.
- Wang, C., Li, H., Chen, W.-C., *et al.* (2019). Propensity score-integrated power prior approach for incorporating real-world evidence in single-arm clinical studies. *Journal of Biopharmaceutical Statistics*, **29**, 731–748.
- Zhao, Z. (2004). Using matching to estimate treatment effects: Data requirements, matching metrics, and Monte Carlo evidence. *The Review of Economics and Statistics*, **86**, 91–107.